SUMMARY OF DISCHARGE DEPOSITS IN THE AMARGOSA VALLEY

By J.B. PACES, J.F. WHELAN, R.M. FORESTER, J.P. BRADBURY, B.D. MARSHALL, and S.A. MAHAN,
Environmental Science Team, Earth Science Investigations Program,
Yucca Mountain Project Branch, WRD, Denver, CO

USGS Milestone Report SPC333M4 to DOE-YMPSCO
Date of Submittal: August 29, 1997

USGS
science for a changing world

SUMMARY OF DISCHARGE DEPOSITS IN THE AMARGOSA VALLEY

This report presents data collected in FY97 and provides a summary of these and previously obtained data from sites of past ground-water discharge located generally down-gradient of Yucca Mountain in the Amargosa Desert and vicinity. Results of this work provide strong evidence that the fine-grained, carbonate-bearing deposits are associated with past discharge of regional saturated-zone ground water. Depths of the present-day potentiometric surface throughout this area vary from around 100 m at past discharge sites in the Crater Flat vicinity, to about 10 m in the Franklin Well area to the south (Fig. 1). These deposits record higher water table elevations that can be linked to periods of increased recharge in up-gradient areas that are, in turn, driven by millennium-scale climate variations. The ultimate goals of these studies are to estimate the response of the saturated-zone to conditions of increased precipitation, recharge and flow related to future pluvial climate conditions. Without this information, the ability of saturated zone flow and transport models to predict hydrologic conditions under future climate states will remain untested.

TABLE OF CONTENTS

1. Current status

1.1 Summary of discharge data

Studies of past discharge deposits in the Amargosa Desert-Yucca Mountain vicinity over the last several years have resulted in reconnaissance-level understanding of the history of activity, the source of water, environmental conditions, and the dynamic nature of the saturated zone response to climate variations over the last 200 ka.

Marsh and wetland deposits associated with ponds, flowing springs and seeps are dispersed widely throughout the Amargosa Desert south of Yucca Mountain. Widely dispersed sites were discharging synchronously during portions of the last two pluvial periods between 9 to 20 ka, 30 to 60 ka, and 90 to 190 ka. These ages, determined by a combination of ^{14}C, U-series disequilibrium, and thermoluminescence methods, contrast strongly with early-held beliefs that discharge activity was of much greater antiquity (early Pleistocene to Tertiary ages). Older cycles of discharge are probably present as well, but they remain unexposed at depth as coring activities have yet to be initiated. Periods of discharge are closely associated with the wettest portions of pluvial episodes rather than the coldest portions that occurred at the height of continental glaciation.

The nature of past discharging waters is central to their importance for hydrological interpretation. Diatom assemblages in many of the deposits show similarities to modern taxa found in silica-rich, possibly warm (<30°C), alkaline springs associated with volcanic terrains. However, authigenic calcite at the same sites show a limited range of $\delta^{18}O$ values of about 19 ± 1‰ for samples least affected by surface evaporation. These values are greater than those

from carbonates associated with deeply circulating ground water discharging from the carbonate aquifer at modern springs. Data from the Amargosa sites suggest cooler water temperatures (<20 to 25°C), recharge at lower elevations, or both, relative to modern recharge areas supplying large-discharge springs.

Isotope data (initial $^{234}U/^{238}U$, $\delta^{87}Sr$, and $\delta^{13}C$) rule out a surface-water source for these deposits. Data also exclude the likelihood of sources from perched aquifer systems recharging through the adjacent hillslopes. Instead, regional, saturated-zone ground water most likely supplied discharge during pluvial episodes. This conclusion requires the regional water table to fluctuate up to about 100 m between the last two glacial and nonglacial periods. In addition, pluvial climates supported seasonal or perennial runoff in the upper portion of Fortymile Wash that would have provided a source of focused recharge adjacent to Yucca Mountain. It is likely that not only did water table elevations increase during pluvial periods, but also that potentiometric surface gradients may have tilted to favor a more westerly flow component into Crater Flat.

The discharge record correlates to other climate proxies in the region and reflects a response of the saturated zone to climate-induced changes in effective moisture, net infiltration, and recharge in source areas. These data do not support the concept of a monotonically declining regional water table driven by tectonic factors (e.g., lowering of the Death Valley base level and increasing the rain shadow effect due to uplift in the Sierra Nevada and Transverse Ranges to the west). Wetter, pluvial conditions were common for a substantial portion of the last 200 ka and are likely to recur in the future along with associated higher water tables.

1.2 Significant uncertainties

In spite of this level of understanding, several important areas of uncertainty remain regarding saturated zone flow paths and transport volumes. The saturated zone hydrologic model is based on present-day structures, rock properties and potentiometric surfaces. The former attributes will remain invariable for long periods of time; however, the latter hydrodynamic property will change under future recharge conditions. The transient nature of the saturated zone water levels is exemplified by hand-dug water wells constructed late in the last century that had become dry prior to significant pumping in the Amargosa Farms area. This period corresponds to a century-scale trend of increasing aridity in the region. Data presented below indicate that down-gradient flow paths during pluvial conditions are still highly uncertain. Although the discharge deposits are closely linked to variations in climate affecting surface infiltration in recharge areas, the time lag between initiation of increased recharge and the higher water table response, as well as the amount of additional recharge necessary to induce high water table elevations remains speculative.

The ability of the SZ hydrologic model to reliably predict future conditions must be further tested by additional information determined from past discharge sites. This information includes a better evaluation of the flow paths associated with discharging ground water as well as the volume of discharge during pluvial episodes. Past flow path issues are best addressed by close coordination with the SZ hydrochemistry program and by drilling several additional shallow water wells at past discharge sites and points intermediate to the mountain. Evaluation of past discharge volumes may be addressed by examining active discharge areas (Ash Meadows, Franklin Lake Playa, Kawich Playa) to determine the relation between modern discharge volume and extent of active deposition. The extent of past discharge deposits can then be used to provide an estimate of past discharge volume that can be compared to results from the SZ model. In addition, if earth orbital dynamics are drivers of climate change throughout the Quaternary, we have yet to test the discharge cycle that most closely represents the next pluvial cycle. Cores drilled through the discharge sites as part of water sampling would provide a means of looking at the vertical extent of deposits with ages of 400 to 350 ka so that they could be compared with the ultimate and penultimate pluvial cycles exposed at the surface.

2. New Data

Data collected in FY97 concentrated on obtaining additional stratigraphic detail in areas previously examined only briefly. In particular, the area near the confluence of the Fortymile and Amargosa systems along the Nevada-California border (State Line deposits) has been the focus of more detailed sampling. This area is particularly important due to its location down-gradient from Yucca Mountain at the toe of the Fortymile Wash alluvial fan. Samples were collected from several new

stratigraphic sections between Franklin and Scranton Wells. Data include new geochronological, isotopic and paleontological data. Additional geochronological data were collected from the Lathrop Wells Diatomite (LWD), Crater Flat Wash (CFW) and Crater Flat deposit (CFD) to better resolve ages and environments within these deposits.

In addition to work on discharge sites, geochronological data from Fortymile Wash alluvial deposits have been completed and provide a history of aggradation and erosion cycles that correspond to variations in surface water over the last two pluvial cycles. Although they are not associated with discharge, these data indicate that Fortymile Wash most likely behaved as a seasonal or perennial stream during pluvial episodes that was capable of moving large amounts of detritus. This water undoubtedly focused local recharge along the upper reaches of the stream providing a ground water mound that may have affected potentiometric-surface gradients beneath Yucca Mountain.

Stable isotope studies of carbonates from spring discharge deposits provide constraints on the recharge source and nature of the aquifer flow path ($\delta^{13}C$), the temperature of discharge($\delta^{18}O$), and supply a limited insight into the climate affecting recharge ($\delta^{18}O$). Stable C and O isotopic compositions were determined from carbonate-bearing samples collected during FY97 from LWD, CFD, CFW, and the State Line Deposits (SLD) at Mesquite Wash, Amargosa River snail site and Scranton Well localities. Of these, only the Scranton Well locale is new and only new data from SLD increase the previously determined $\delta^{13}C$ and $\delta^{18}O$ ranges. The new data suggests that (1) evaporation has affected water and carbonate isotopic compositions during deposition of the deposits at the State Line area, and (2) the Scranton Well section carbonates are remarkably similar to primary carbonates from the LWD and CFD deposits described in Paces and others (1996).

2.1 State line area

2.1.1 Franklin Well – Mesquite Wash Section

An extensive area located at the toe of the Fortymile Wash alluvial fan consists of fine-grained deposits lacking alluvial sediments. This broad gently sloping terrace is elevated with respect to present-day drainage channels associated with both Fortymile Wash on the north and the Amargosa River on the south (Fig 2). Exposure into this series of deposits is best expressed on its southern end near Franklin Well where a south-southwest trending arroyo has incised about 6 m into the terrace-forming deposits (Fig. 2). A large, isolated mesquite tree at the mouth of this arroyo provides a landmark identifying its location as well as the informal name used here.

Cliff-forming walls about half-way up the arroyo expose a series of stratified fine-grained deposits consisting of greenish to buff-colored muddy silts and fine sands with variable amounts of authigenic cements (Fig _), primarily calcite as well as lesser gypsum, silica and halides that may or may not be primary. Efflorescing salts with salty to bitter tastes are most notable in the lower beds below unit 8 in Fig. 3. A 5-m-thick section at the same site shown schematically in past reports (Fig. 13a of Paces et al., 1996) on the west wall of the arroyo was measured and sampled for isotope, geochronological, and paleontological studies.

2.1.1.1 U-series disequilibrium: Three samples (HD2198, HD2199, and HD2200) of well cemented silty sediment from units B and D in the lower part of the section (Fig 3) were analyzed for U and Th isotopes (Table 1; analytical techniques given in Appendix 2 of Paces et al., 1996). U contents in these samples are low (0.2 to 0.7 ppm) and Th contents are high (0.5 to 2.7 ppm) resulting in atomic Th/U ratios of 2.7 to 6.2. As a consequence, $^{232}Th/^{238}U$ activity ratios vary from 0.89 to 2.0. These large values preclude accurate estimation of the ^{230}Th that was inherited at or subsequently the time of cement formation, and thus reliable $^{230}Th/U$ ages for these samples cannot be determined. The origin of high Th contents relative to U is apparently not related to the abundance of silt- and sand-sized detrital material as the observed cement/detritus is approximately the same as other nodular carbonate samples with much lower Th/U ratios. Instead, elevated Th along with abundant halides in these units may indicate that saline, alkaline waters were present during or after sediment deposition. Enhanced Th^{4+} stability has been demonstrated in alkaline lakes in the western US (Anderson et al., 1982; Simpson et al., 1982; LaFlamme and Murray, 1987). Therefore, ground water, or a combination of ground water and surface water acting in discharging playa setting, may have provided elevated levels of dissolved Th relative to more typical conditions favoring dilute waters.

Although $^{230}Th/U$ age estimates are not possible for these samples, measured $^{234}U/^{238}U$ activity ratios greater than unity indicate that ages are probably not much older than middle Pliestocene (several hundred thousand years). These ratios are also correlated with stratigraphic position (and hence age) with values of about 1.2 for the lowermost unit (B in Fig. 3) and values of between 1.7 to 2.0 for the hard, massive unit D. Values for both units are less than $^{234}U/^{238}U$ activity ratios measured for units at higher stratigraphic levels (2.6 to 3.6 for samples above unit 8). Although detritus-corrected $^{234}U/^{238}U$ were not calculated for these high $^{232}Th/^{238}U$ samples, $^{234}U/^{238}U$ model ages based on an assumed initial $^{234}U/^{238}U$ ratio of between 3.0 and 3.1 (Paces et al., 1996) are about 800 ka for unit B and 250 to 350 ka for unit D. These model ages are clearly over-estimates of true ages because some detrital correction is necessary and will yield higher $^{234}U/^{238}U$ ratios for the hydrogenic component, and thus a younger model age. Older ages implied by $^{234}U/^{238}U$ activities in these samples are supported by thermoluminescence ages from intercalated units presented below.

Samples from above the thick, ledge-forming unit 8 yield finite $^{230}Th/U$ ages from 101 to 182 ka and initial $^{234}U/^{238}U$ activity ratios from 3.3 to 3.9 that are correlated with age. These ages are inconsistent with those obtained previously from plant petrifactions from unit 8 ($^{230}Th/U$ ages of 97 to 105 ka) and the thermoluminescence age of about 26 ka (TL-45) from an intermediate silty unit (Paces et al., 1996). The correlation between age and initial $^{234}U/^{238}U$ ratio is apparent on a ^{234}U-^{238}U-^{230}Th plot as a subhorizontal array of points with increasing $^{230}Th/^{238}U$ and constant $^{234}U/^{238}U$ (Fig. 4). This trend occurs if samples have undergone recent U loss resulting in increases in $^{230}Th/^{238}U$ with little change in $^{234}U/^{238}U$. This effect has been noticed before (Paces et al., 1996), but not as dramatically as in this suite of low-error subsamples from the same horizon. The effects of U loss can be removed if the initial $^{234}U/^{238}U$ is known *a priori*. A $^{234}U/^{238}U$ model age that is not dependent on the $^{230}Th/^{238}U$ ratio can be then be calculated using the assumed initial $^{234}U/^{238}U$ ratio. In this case, previously analyzed materials (HD1711, HD1854, and HD1737) both above and below the horizon containing HD2201 and HD2202 have well defined initial $^{234}U/^{238}U$ activity ratios between 3.0 and 3.1 (Paces et al., 1996). Using a value of 3.05, model $^{234}U/^{238}U$ ages for HD2201 and HD2202 vary between 49 and 66 (Table 1). This range expands slightly to between 40 and 75 ka if initial $^{234}U/^{238}U$ values of 3.0 and 3.1 are used. Although this age range is slightly older than that of TL-45, the model ages are generally consistent considering the overall uncertainties in both the TL determination and the assumed initial $^{234}U/^{238}U$.

Several additional samples (HD2203 to HD2205) of carbonate containing varying amounts of silica were collected from the broad, carbonate-capped terrace surface about half a kilometer north of the head of Mesquite wash (High Terrace on Figure 2). These samples were either collected from the surface, or from shallow (~10 to 20 cm deep) excavations from broad (50 to 100 m diameter) mound-like landforms up to 1 m higher than the surrounding surfaces. Individual clasts consist of sand-free massive to finely laminated carbonate often with pancake-like morphologies similar to algal structures. U-series data for these samples failed to produce high precision ages in spite of their clean looking appearance. The several samples that have smaller uncertainties are old relative to the high terrace surface at the Mesquite wash section. Calculated $^{230}Th/U$ ages for these materials vary between about 140 and 450 ka. These old ages are not the artifact of recent U loss as described above. Measured $^{234}U/^{238}U$ activity ratios are generally less than 2.0, indicating *in situ* decay from typical ground water $^{234}U/^{238}U$ values of 3.0 or greater. Therefore, $^{230}Th/U$ evidence suggests that although this part of the discharge system was active in the Pleistocene, it may not have been active throughout the last pluvial episodes.

A single sample of hectorite (HD2206), a trioctahedral member of the montmorillonite clay group, ore from a clay pit on the south side of the Amargosa River near Franklin Well (Fig 2) was analyzed for U-Th isotopes. Further east in the Amargosa Flat area north of Ash Meadows, clay-rich deposits are intercalated with ash beds dated between 2 to 4 Ma (Hay et al., 1986). Ages for clay deposits elsewhere in the area are commonly assumed to be of similar age; however, the hectorite pit south of Franklin Wells is located in an alluvial fan slope setting in contrast to the playa settings for other Pliocene clay deposits to the east. Isotopic results indicate that the hectorite ore has a Pleistocene bulk age. The single analysis of fine-grained, massive, white, porcelaneous material has a $^{230}Th/U$ age of 235 ± 41 ka and an initial $^{234}U/^{238}U$ of 3.3 ± 0.3,

identical, within error, of undisturbed ground water carbonates in the Mesquite Wash area.

2.1.1.2 Thermoluminescence: Two additional thermoluminescence samples were collected from the lowermost sediments at depths of 480 (TL-84) and 525 (TL-85) cm below the upper terrace surface (Fig. 3). As with U-series analyses from these same beds, TL samples showed some anomalous behavior. Thermoluminescence response for TL-84 exhibited two different types of luminescence. One of these was a stable TL peak (around 250-350°C) and the second, a sort of photoluminescence around 350-500°C. Discrimination between these two types of luminescence response is necessary to obtain a signal that can be clearly related to the energy released from the age-dependent accumulation of trapped electrons. Therefore "sunlight" experiments were performed to further test the luminescent properties of the sample. Photoluminscence initially increases by exposure to sunlight, followed by a weakening after about 20 hours of exposure and is completely drained off after about 32 hours in sunlight. These results indicate that the luminescence observed at higher temperatures is caused by different processes than those responsible for the signal that is relevant to dating. All TL ages for these samples are derived from temperatures in the 300-350°C stable TL range.

These samples also have a wide range of moisture contents. Field moisture, determined from material as sampled in the field, is low (~ 2% by weight); however both samples have the capacity to retain large amounts of water with a saturated moisture content of TL-84 up to 77% by weight. Water in pore space will reduce the dose rate to the silt grains and thus affect the TL age. Ages calculated using dose rates determined for three different water contents are given in Table 2 including field content, saturation content and an arbitrarily selected value at half of the saturation value. The range in TL ages thus obtained is from 98 to 184 ka for TL-84 and 149 to 279 ka for TL-85. These ranges are much larger than error ranges estimated from analytical uncertainty (about 10%). The ages calculated at half-saturation moisture contents (142 ± 11 ka and 216 ± 24 ka) are interpreted to be the most reasonable given the likely history of ground water saturation at this site. Therefore, it is probable that these TL ages reflect discharge activity associated with high water tables during the penultimate (OI[1] Stage 6) pluvial cycle. However, the error range based on analytical uncertainties undoubtedly underestimates the true uncertainty in the quoted age given the unknown moisture history. Both of these ages are older than the previously obtained values of 94 ± 18 ka and 26 ± 3 ka for TL-44 and -45, respectively (Paces et al., 1996), for units higher up in the section.

2.1.1.3 Stable Isotopes: Whole rock carbonate $\delta^{13}C$ and $\delta^{18}O$ values were determined from calcareous portions of the Mesquite Wash section (Figures 5 and 6a). Whole rock determinations average all sources of calcite within a sample (authigenic, detrital, pedogenic, and biogenic). Variable proportions of these components will create a mixed signal that may not carry as much information as that in the individual components. Although future work will isolate authigenic inorganic and biogenic components, whole rock data presented here shows a bimodal distribution. The basal portion of the sequence has relatively constant $\delta^{13}C$ and $\delta^{18}O$ values of about -1.5 and 20‰, respectively, whereas the higher levels contain slightly ^{13}C-enriched and markedly ^{18}O-enriched isotopic compositions. These enrichments are consistent with CO_2 evasion and evaporative enrichment of the water prior to carbonate precipitation and suggest local ponding of discharge or runoff waters. Such $\delta^{13}C$ and $\delta^{18}O$ variations are not consistent with increases in either pedogenic or detrital components.

Figure 6a indicates that the onset of increased evaporative enrichment may have been roughly coincident with the termination of the penultimate glaciation (OI Stage 6) at around 130 ka. The presence of carbonate early during the following interglacial (OI Stage 5) as well as the deposition of several meters of sediment suggests that the site was still marsh-like during this interval.

Stable isotopic indications of evaporative processes in the sequence are roughly coincident with exceptionally high Sr concentrations in the same materials (see below), corroborating salinity increases at that time. They are not, however, coincident with the occurrences of sulfate or halide salts deeper in the section. Indeed, the stable and Sr concentrations of

[1] Oxygen Isotope - cyclic variations of $\delta^{18}O$ based on analysis of deep sea sediments define a pattern of peaks and valleys, numbered as stages, that correlate to glacial episodes (Imbrie et al., 1984).

that portion of the section indicate relatively dilute water chemistries. This suggests that those salts are probably not primary, but may have concentrated in the arroyo walls from sediment porewaters evaporating at the wall of the arroyo, or were introduced after sedimenation but before exhumation (e.g., during subsequent interglacial deposition).

Youngest carbonate in the sequence, deposited between 30 and 50 ka, has the lowest $\delta^{13}C$ value of about -4‰ and a $\delta^{18}O$ of -21.6‰ (Fig. 6a). These values are similar to but slightly ^{18}O-enriched with respect to values from the capping marly carbonates reported previously (Paces et al., 1996). The lower $\delta^{13}C$ value suggests that input of Paleozoic carbon, either from regional ground waters or from interactions with detrital components in an alluvial aquifer, was less during the ultimate pluvial cycle (OI Stage 6).

2.1.1.4 Strontium Isotopes: Strontium isotope compositions vary substantially between ground waters associated with the Fortymile Wash and Amargosa Valley flow systems (Peterman and Stuckless, 1993). Fourtymile Wash $\delta^{87}Sr$ values are restricted between about 1.1 and 4.0‰, whereas ground waters in throughout the Amargosa Desert attain much larger values as great as 10 to over 20 ‰. The source for the more abundant radiogenic Sr in the Amargosa system is presumably related to Precambrian clastic rocks with relatively large Rb/Sr ratios in the northern Funeral Mountains. If ground waters associated with these two systems interact in the lower reaches of the Fortymile alluvial fan, evidence of the interaction should be preserved in $\delta^{87}Sr$ in the mixed waters or in carbonates derived from these waters. The presence of the two aquifers may be reflected in modern waters in the Amargosa Farms region where the shallow aquifer tends to have low $\delta^{87}Sr$ values of 3 to 4.5 ‰ whereas deep wells tend to sample waters with larger $\delta^{87}Sr$ between 7.8 to 13 ‰ (Peterman, written communication).

Samples of SLD carbonate-rich materials were analyzed for Sr isotopic compositions and concentrations. Powdered splits from the same subsamples analyzed for U-Th isotopes were weighed and leached with dilute HCl. Leachates were spiked for isotope dilution and residues were dried and re-weighed to determine the mass of the carbonate removed. Therefore, Sr concentrations reported in Table 3 represent the authigenic cements without dilution from silicate components.

Resulting $\delta^{87}Sr$ values for SLD samples span a range between 10.4 and 12.2 ‰ and Sr concentrations vary between 51 and 1940 ppm (Table 3). These values are similar to those reported earlier from this area (Paces, 1995) although the whole rock Sr contents in that report do not replicate the low values presented here. Samples from the Mesquite Wash section show a pattern of correlation between reciprocal concentration and $\delta^{87}Sr$ (Fig. 7) of the type commonly attributed to binary mixing. Two of the three subsamples (HD2203-A and -B) from the high terrace deposits north of Mesquite wash fall on the same trend; however, the third, from a separate sample (HD2204), shows a much higher $\delta^{87}Sr$ at an intermediate Sr concentration. Although not collinear, the eight Mesquite Wash section subsamples have linear regression r^2 values between about 0.89 and 0.94 depending on whether or not the lowest concentration sample is omitted.

The anti-correlation of Sr concentration and isotopic composition also shows a systematic variation with depth in the section (Fig. 8). Cements in the stratigraphically highest two samples (HD2201 and HD2202) have the greatest concentrations with the smallest $\delta^{87}Sr$ values whereas samples from the lowest part of the section have greater $\delta^{87}Sr$ but most noticeably much lower concentrations. Measured Sr concentrations of 51 to 111 ppm in cements of unit D (Fig. 3) are comparable with Tertiary lacustrine limestones of Bat Mountain although $\delta^{87}Sr$ values in the limestones are only 3 to 6 ‰ (Paces, 1995). The stratigraphic correlations noted here are consistent with results from reconnaissance samples reported previously (Paces, 1995) indicating a trend towards lower $\delta^{87}Sr$ in the upper units (samples HD1706, HD1710 and HD1711) of the wash and higher $\delta^{87}Sr$ and lower concentrations in the lower units (HD1708).

Lack of precise geochronology limits the stratigraphic interpretations that can be gleaned from the available Sr data from the State Line deposits. The data are clearly linked to a ground water source containing a significant contribution from radiogenic Sr present in the Amargosa Valley. The smaller $\delta^{87}Sr$ values in deposits formed between 30 to 50 k.y. may be related to increased amounts of lower $\delta^{87}Sr$ from the Fortymile Wash system during that time, relative to the larger $\delta^{87}Sr$ and smaller concentrations in calcite formed during drier periods. However, until additional data are available, patterns relating to the

timing and degree of interaction between the two hydrologic systems remain speculative. The very small Sr concentration values for unit D in the lower part of the section appear unique for data from ground water discharge deposits. Their similarity to lacustrine limestone values may provide further support of the possibility that dilution of ground waters by surface runoff was involved in the genesis of at least some of the horizons within this deposit.

2.1.1.5 Paleontology: The siliceous marls and sands that comprise the spring deposits in Mesquite Wash area of the State Line deposits locally contain abundant diatoms. Lenses of diatom-rich marl occur in the upper third of the exposure, generally 50- to 100-cm below the crumbly, limestone cap at the top of the section. The characteristic taxon in these lenses is *Denticula valida*, which also dominates much of the Lathrop Wells deposits. Some samples from Mesquite Wash contain common *Achnanthes thermalis*, a diatom living in hot springs and that indicates a thermal water component to the spring deposits at State Line. The common presence of *Rhopalodia acuminata* indicates that the spring water was alkaline-enriched, modestly saline (above 500 ppm TDS), and high in silica. The diatom assemblage, along with abundant silicified plant fossils in some beds, indicates that discharge contained a significant hydrochemical signature derived from water-rock interactions along a volcanic rock-dominated flow path.

2.1.2 Franklin Well – Snail Site Section

Greenish brown muddy silts comprise a flat, low terrace above the modern Amargosa River channel (area surrounding Snail Site in Fig. 2) and inset into the carbonate-capped upper terrace that constitutes much of the lateral extent of the State Line deposits. These fine-grained deposits contain aquatic and terrestrial molluscs dated previously at 9.0 to 10.2 ka by radiocarbon and 11 ± 2 by $^{230}Th/U$ methods (Paces et al., 1996). The initial $^{234}U/^{238}U$ activity ratio of 3.3 for the aquatic snail shell is within error overlap of values from undisturbed materials in the upper portions of the Mesquite Wash section.

These deposits are not well exposed by channel incision and their vertical extent is unknown. A 500 cm deep hole was hand-drilled into the non-lithified sediments, and select auger intervals were sampled for paleontological study. The entire hole contained fine-grained clastic sediments varying from silty sand to sandy mud. One bucket (number 22) contained minor small carbonate nodules, but it is unclear whether they are authigenic or clastic. Coarser sands and gravels are entirely absent from the 500 cm core indicating that in spite of the proximity to the modern Amargosa river channel, fluvial sedimentation similar to that occurring in the channel today did not control past sedimentation at this the hole. Sediment appeared saturated with water at a depth of about 350 cm; however deeper material became drier, and no water entered the hole during boring. The hole bottomed in the silty deposits and their total depth remains unknown.

2.1.2.1 Thermoluminescence: Sample TL-86 was obtained from a depth of 320 cm in the auger hole by shielding the auger bucket from sunlight as it was retrieved from the hole. The sample had a relatively high field moisture content (17% by weight) that is consistent with the wet sediment retrieved from between about 330 and 350 cm. Dose rates were obtained by analyzing bulk material for K, U, and Th in the laboratory rather than *in situ* because of the large diameter of the radiation detector. The resulting dose rate is likely to be representative of the in situ radiation field due to the deposit's homogeneous, fine-grained nature. The value of 5.5 Gy/year is within 1.5% of an *in situ* value measured in the same sediments at a depth of about 40 cm (TL-46, Table 9 in Paces et al., 1996). The resulting half-saturation total bleach age of 14 ± 1.3 ka for TL-86 is similar to, but slightly older than, the age obtained from TL-46; however the uncertainty in saturation effects do not allow clear age resolution. Both values are only slightly older than the 9 ka calibrated ^{14}C ages obtained from terrestrial snail shells at the top of the section. These data indicate a relatively large sediment accumulation rate within the small basin. If the Amargosa River occupied a position similar to its present course during the late Pleistocene, eolian sediment supply could have been augmented by an over-bank fluvial source of fine, but not coarse, clastic sediment.

2.1.2.2 Stable Isotopes: Nine of the intervals sampled in this auger hole were calcareous. These samples have whole rock $\delta^{13}C$ and $\delta^{18}O$ values shown in Figure 6b. Much if not all of the auger section from this site appears to postdate the nearby Mesquite Wash sequence but it is clear that the two sections are not the same age and do not have the same depositional environment. Nonetheless, the $\delta^{13}C$ and $\delta^{18}O$ values of these samples appear compatible with conditions recorded by the younger

portion of Mesquite Wash sequence. Calcite $\delta^{13}C$ values average around -3‰, similar to the latest part of the Mesquite Wash sequence. The $\delta^{18}O$ values are variable, ranging from about 19 to over 24‰, suggesting intermittent ponding and evaporation of discharge waters. For example, bucket 6 (60 cm depth) has both ^{18}O-enrichment and an ostracode assemblage suggestive of higher salinity waters.

2.1.2.3 Paleontology: Preliminary analysis of selected intervals indicate diatoms are common to abundant in the upper 400 cm of the section. The diverse diatom assemblage is characterized by freshwater benthic species common in alkaline-enriched waters and indicating the past presence of a through-flowing marsh. There is some diatom assemblage overlap with the deposits of the high terrace at Mesquite Wash that suggests the Amargosa marsh system was fed in part by groundwater discharge of similar chemistry. However, the diatom assemblage of the low terrace marsh deposits indicates generally fresher water with a higher humic content that was probably derived from decaying marsh vegetation.

The ostracode assemblage in the upper 10 cm indicates an environmental setting consisting of a wetland with flow through it and containing cold freshwater. By contrast, at around 60 cm ostracode assemblage indicates a slightly saline wetland having waters whose solutes are alkaline enriched. Alkali enrichments imply the solutes have been derived from volcanic water-rock interactions. The ostracode assemblage around 100 cm implies a low flow possibly ephemeral wetland that, if *L. hericki* was present, existed under relatively cold climates. The remaining materials found in the samples below 110 cm indicate a probable marsh setting having variable levels of surface water that range from short seasonal inundation to shallow ephemeral wetlands and or pools associated with local spring or ground-water discharge.

2.1.3 Scranton Well Section

Flat-lying carbonate-capped discharge deposits underlie an extensive area to the northwest of Franklin Well. A 150 cm diameter by 600-cm deep well was dug to the water table by hand around the turn of the century to provide water for the Scranton Site along the old Tonapah and Tidewater Railroad (Fig. 2). The well is still open and although dry, it allows vertical access to the upper six meters of these deposits (Fig 10).

Sediments are generally similar to those at Mesquite Wash and consist of fine-grained clastic materials lacking substantial internal bedding interbedded with buff-colored dense limestones and zones containing coarse carbonate nodules. As elsewhere in the State Line deposits, gravels characteristic of higher-energy alluvial environments are completely missing. Sixteen samples, biased toward carbonate-bearing strata, were collected from the walls of the well at approximately 30 to 40 cm intervals.

2.1.3.1 U-series disequilibrium: Eight analyses from the four uppermost Scranton well samples have been completed. All but one of these analyses are from subsamples of matrix areas of buff to light pink limestone with between 15 to 30 percent fine sand by volume. Although analytical uncertainties for $^{230}Th/^{238}U$ and $^{234}U/^{238}U$ are less than about one percent of the value reported, Th abundances are high ($^{230}Th/^{232}Th$ activity ratios between 2.5 and 4.1) resulting in large uncertainties in the detritus-corrected ratios. As a result, uncertainties in calculated age and initial $^{234}U/^{238}U$ activity ratios are large (large error ellipses in Fig. 11). In spite of this, ages and initial $^{234}U/^{238}U$ ratios cluster together for subsamples "a" and "b", as well as "c1" and "c2". Therefore, late Pleistocene ages of 40 to 60 ka and 80 to 90 ka seem reasonable for the upper 1.2 m of this section.

One analysis of a 2 mm thick banded travertine vein (HD2208b-1) within the limestone had the highest U content (4.5 ppm) and lowest Th (0.14 ppm) resulting in a $^{230}Th/^{232}Th$ activity ratio of 127. Consequently, age and initial $^{234}U/^{238}U$ values for this material (59.2 ± 0.9 ka and 3.19 ± 0.02, respectively) are much more precise than matrix materials. Bulk rock data from the same sample has a $^{230}Th/U$ age of 106 ± 18 ka, but an elevated, albeit imprecise, initial $^{234}U/^{238}U$ activity of 5.0 ± 1.9. Correction for U loss using an assumed initial ratio of 3.2 gives a negative model $^{234}U/^{238}U$ age. However use of an initial ratio of 4.5 (Table 1), similar to calculated values from subsamples "c1" and "c2", yields a model $^{234}U/^{238}U$ age of 54 ka overlapping the age of the included travertine vein.

2.1.3.2 Stable Isotopes: Whole-rock $\delta^{13}C$ and $\delta^{18}O$ values of calcite-rich samples from the Scranton Well sequence are remarkably constant (Fig. 6c). Calcite $\delta^{13}C$ values cluster at -1 ± 1‰ and $\delta^{18}O$ values at about 19.5 ± 1‰. These values form a relatively tight group that is isotopically similar to the

"primary" carbonate from the LWD and CFD deposits (Fig. 5). At these sites, carbonates least likely to have been affected by evaporation or diagenesis clustered around $\delta^{13}C$ and $\delta^{18}O$ values of 0-2 and 19‰, respectively. These compositions were assumed to be most indicative of the chemistry and temperature of the discharging fluids (Paces et al., 1996). The similarity of the Scranton Well section carbonates to the deposits on the north side of the Amargosa valley as well as to those in the lower half of the Mesquite Wash sequence suggests they are all related to regional-scale rather than localized groundwater sources.

2.2 Lathrop Wells Diatomite

2.2.1 Station 6 section

2.2.1.1: U-series disequilibrium: The stratigraphic section at Station 6 (Fig 12; Paces et al., 1996) provides the most complete, unambiguous stratigraphy within the main badlands area at the Lathrop Wells Diatomite deposit. Additional samples from the base of the diatomite unit as well as the green sand unit have been analyzed by U-series (Table 4) to better constrain ages on these older horizons.

Four additional samples of small plant petrifactions from the base of the white diatomite bed result in ages between 33 and 101 ka with initial $^{234}U/^{238}U$ activity ratios between 3.88 and 4.7. Two of the subsamples (HD1970-U3 and -U6) relatively high ^{232}Th contents resulting in large detrital corrections and elevated initial $^{234}U/^{238}U$ activity ratios with large uncertainties (Fig. 13). Subsample HD1970-U5 has similar Th contents (about 5 ppm) but much higher U concentrations (13.5 versus 4 to 5 ppm). The calculated $^{230}Th/U$ age (33 ± 2 ka) is similar to the more-precise of two previously obtained ages (42 ± 2 ka; Paces et al., 1996) as is the initial $^{234}U/^{238}U$ activity ratio (3.88 ± 0.13 compared to 3.86). These initial ratios are also identical to 14 to 16 ka materials analyzed previously (HD1385-1 and HD1969 on Fig. 13). An additional subsample (HD1970-U4) has a much greater age and initial $^{234}U/^{238}U$; however, its model $^{234}U/^{238}U$ age of 30 ka assuming an initial ratio of 4.0 suggests that this specimen has also suffered U loss in the recent past. Therefore, the best estimate of the $^{230}Th/U$ age of the base of the diatomite bed is interpreted as between 33 and 42 ka.

Similar small plant petrifactions as well as nodular carbonate occur in the upper 20 cm of the underlying green sand unit. One of three new analyses (HD1971-U4) has a reasonably well-defined age of 50 ± 5 ka and an initial $^{234}U/^{238}U$ activity ratio of 3.66 ± 0.12. This analysis is much younger than two previously obtained ages of 115 and 152 ka from the same horizon (Paces et al., 1996). Two other analyses have much lower uranium concentrations and $^{230}Th/^{232}Th$ ratios yielding results with very large uncertainties. These two analyses can be interpreted to have ages of 112 and 132 ka if assumed initial activity ratios are as great as 4.4, or 25 and 45 ka if initial ratios are similar to HD1971-U4 (i.e., 3.66). Neither biotubation of younger clastic material into older sediments nor sediment reworking of older plant petrifactions into younger sediments can be excluded as possible explanations of the two possible age populations. Because of the scattered results, the age of this horizon remains poorly constrained.

Four additional samples of nodular carbonate from the exposed base of the green sand unit yield a range of ages and initials that are, in part, best interpreted as the results of U loss. Subsamples HD1972-U2r and -U4 have model $^{234}U/^{238}U$ ages of 178 and 185 ka using initial ratios of 3.65 and 3.60, respectively. These model ages are nearly coincident with two previously obtained $^{230}Th/U$ ages of 187 and 173 ka (Paces et al., 1996). Subsample HD1972-U3 yields a model $^{234}U/^{238}U$ age of 179 ka using an initial $^{234}U/^{238}U$ activity ratio of 3.9; intermediate between the former values and the 4.6 ± 0.6 value obtained along with the $^{230}Th/U$ age of 180 ± 14 ka from HD1972-U1r.

The older ages for the green sand unit are supported by $^{230}Th/U$ and model ages from other samples within the green sand unit in the main badlands area. Six additional samples show some effects of U loss, but yield consistent $^{230}Th/U$ or model $^{234}U/^{238}U$ ages between about 90 and 185 ka with observed or assumed initial $^{234}U/^{238}U$ activity between 3.0 and 4.6 (Table 5). Terrestrial and aquatic molluscs were found at one of the green sand unit localities (Paces et al., 1996). These fossil shells have conventional ^{14}C ages between 35 and 42 ka representing about 1.2 to 0.5 percent modern carbon. Small amounts of recrystallization and exchange with younger carbon could cause the otherwise "dead" radiocarbon signatures of these shells to appear dateable if the deposits in which they occur are truly older than about 100 ka.

2.2.2 Northwest fringe area

Fine-grained deposits are present under a thin veneer of slope-wash colluvium about 400 to 500 m north of the main badlands area (Fig 12). Samples of fine grained materials were collected from surface exposures along the shallow wash at and to the southwest of station 12.

2.2.2.1: Paleontology: An additional sample (96:12:05-1) collected from the N. fringing deposits (from Station 16, about 75 m S. of Station 12) revealed the same diatom dominants, *Denticula valida* and *Epithemia argus*, as found in diatomaceous units of the main badlands deposit. Diatom assemblages in this sample corroborated earlier analyses from the fringe areas of the deposit and supports their correlation to the middle and lower parts of the main badlands area of the deposit (green sand units at stations 6 and 8). Perhaps this tentative correlation suggests that the Lathrop Wells deposits were most extensive at a time that included the deposition of station 8, provisionally dated to between 90 and 160 ka.

2.3 Crater Flat Wash

Vertical exposures are nearly non-existent in the low-relief, flat-lying deposits along the west side of the wash draining Crater Flat. A 380-cm deep hole was augered by hand in the northern portion of the deposit on top of the small mound above station 2 (Fig. 14).

2.3.1. Surface samples

2.3.1.1 Thermoluminescence: Previous geochronology at the Crater Flat Wash site is limited to two $^{230}Th/U$ ages of 15.2 and 19.9 ka from individual rhizoliths collected from lag deposits in the central portion of the exposure (Paces et al., 1996). Sample TL-87 was collected the same area (Fig. 14) immediately underlying one of the rhizolith-bearing hard, green sandy units. Field moisture (7.4%) and saturation moisture (53%) yield a range of TL ages between 15 and 22 ka. The total bleach age of 18 ± 3 ka based on half-saturation is interpreted as a reasonable approximation of the saturation history of the material. The age is consistent with $^{230}Th/U$ ages from the overlying unit.

2.3.2. AUGER-1 section

2.3.2.1 Stable Isotopes: Selected intervals from the nearly 4 meter hole were collected (Fig. 15) and the calcite-bearing samples analyzed for whole-rock $\delta^{13}C$ and $\delta^{18}O$ values (Fig. 5e). The most noticeable aspects of this sequence are an apparent covariance of the $\delta^{13}C$ and $\delta^{18}O$ values and the general ^{18}O-enrichment of the calcite. Both of these are consistent with evaporation and CO_2 evasion from standing or slowly moving water. None of the calcite $\delta^{18}O$ values are as low as those from the LWD, CFD, or Scranton Well sections, suggesting that the CFW deposit may have been an outflow setting allowing discharge sufficient opportunity to interact with the ambient atmosphere.

2.3.2.2. Paleontology: A suite of auger bucket samples from Auger-1 also provides material for diatom analysis to a depth of 360 cm. Although diatoms are absent in several samples, they are common and well preserved at 100-cm depth. Diatoms are also present at 240, 270, 290 and 360 cm. Below 270 cm *Denticula valida* and *D. elegans* are present, whereas above 270 cm *Nitzschia denticula* characterizes the section. *Nitzschia denticula* is a common diatom in Quitobaquito Spring (Organ Pipe Cactus National Monument, Pima County, Arizona). Quitobaquito Spring discharges sodium bicarbonate water with a total dissolved ion concentration of about 700 mg/liter (Carruth, 1996). In general, the diatom assemblages of the CFW locality indicate an alkaline, silica-rich water similar to the hydrochemistry of discharge that formed the Lathrop Wells Diatomite deposits.

The ostracodes given for three intervals in Figure 15 are rare and may or may not be in place. If *P. unicaudata* was present it implies a shallow permanent-to-ephemeral wetland commonly having slightly saline to saline water.

2.4 Crater Flat Deposit

2.4.1 Station 5 auger section

2.4.1.1 Stable Isotopes: Whole-rock calcite $\delta^{13}C$ values from the auger sequence (Fig. 16) increase smoothly with depth, from 0 to about -4‰ (Fig. 6d) at the same time that $\delta^{18}O$ values display a less-pronounced but general trend to higher values (from about 19 to about 20‰). At present, there are no age determinations from this sequence, but ages in the nearby Pit 1 range from about 65 to 10 ka for sediments down to about 100 cm depth (Paces et al., 1996). Carbon data do, however, suggest mixing between volcanic- and Paleozoic carbonate-dominated ground waters. Volcanic aquifers tend to display lower $\delta^{13}C$ values because their main carbon

source is the oxidation of plant organic matter, whereas the Paleozoic aquifers carbon sources are the marine carbonate themselves that generally have values near 0‰. Petrographic studies to determine the nature of the carbonate throughout this sequence are required to verify that these variations are not being caused by changes in the proportions of detrital or pedogenic components.

2.4.1.2 Paleontology: Selected samples from the station 5 auger hole were checked for diatoms. All samples were barren except for one valve of *Cocconeis placentula* from a depth of 100 cm. This is a common freshwater diatom that lives in calcium bicarbonate waters at pH values above 7. Because of its extreme rarity in the sample suite, it probably cannot provide significant information about the chemistry of discharge at CFD.

The ostracode assemblage is composed of rare shell material. The taxa present suggest the paleoenvironmental setting consisted of a shallow wetland or pool complex probably supported by discharge from seeps.

2.5 Fortymile Wash

2.5.1 History of Aggradation/Erosion and Local Recharge to the Saturated Zone.

Although not a site of past ground-water discharge, Fortymile Wash has a significant impact on the water table under Yucca Mountain. Presently, the potentiometric surface under Yucca Mountain dips very gently to the east towards Fortymile Wash with no more than several meters difference between well J-13 and wells along Yucca Crest (Ervin et al., 1993). Past water table fluctuations of over 100 m undoubtedly overwhelmed this small difference. Elevated water tables must have been influenced by variations in local recharge sources with the result that pluvial potentiometric surfaces would not have looked similar to those measured today. The purpose of this section is .to present geochronological evidence supporting the presence of seasonal and possibly perennial flow in the upper reaches of Fortymile Wash. This greater surface flow most likely provided focused recharge to the saturated zone forming a recharge mound beneath the wash axis as far south as Busted Butte.

Fortymile Wash forms a long, remarkably linear alluvial fan extending southward from the mouth of Fortymile Canyon, extending south and broadening out into the central Amargosa Desert (Fig. 17a). It forms the largest and highest drainage basin contributing to the Amargosa River system and heads in the upland areas of Timber Mountain. The historical record of Fortymile Wash shows it to be extremely ephemeral with observed flow during less than 30 days over the past 37 years. However, the fan of Fortymile Wash is one of the largest in the southern Basin and Range Province. The fan surface slopes gently to the east and west, away from the north-south axis, however, the active channel occupies a 10 to 35 m deep, steep-walled arroyo in the upper fan area adjacent to Yucca Mountain. The contrasting geomorphologic features indicate the stream dynamics cycle between episodes of aggradation and incision in order to build upper fan surfaces and then cut down through them.

Deposits associated with the upper fan surface, also called the high terrace, as well as inset deposits associated with incision since the last aggradation event have been dated by U-series disequilibrium (Table 6) and thermoluminescence methods (Table 7). Conclusions in this report are based largely on the former data set, but the thermoluminescence data not presented in Table 7 are generally consistent and provide support to the $^{230}Th/U$ chronology. The upper fan surface was sampled to the south near Gate 510, in the J-13 area, and near the mouth of Fortymile Canyon (Fig 17b). Multiple cobbles containing relatively thin rinds (typically less than several mm) of calcite plus opal were selected from alluvial gravels associated with the uppermost soil horizon. Massive calcite/silica and individual rhizoliths were also collected at several sites. Innermost, silica-rich clast rinds between 0.1 and 0.5 mm were sampled by grinding with carbide dental burs to obtain sample weights between 10 and 100 mg. These samples represent the oldest pedogenic materials within a given horizon and are most likely to reflect close minimum ages to alluvial deposition events. Resulting $^{230}Th/U$ ages for these high terrace deposits range between about 75 and 80 ka at the Gate 510 quarry near where the fan broadens significantly, and between about 50 to 75 ka in the J-13 area. Dates from buried soils place further constraints on the latest deposition of the uppermost several meters of alluvium. These include rhizoliths between about 80 and 100 ka at the Calico Fan and Sever Wash Gooseneck sites. Cumulative data indicate that the latest alluvium was deposited between 50 and 100 ka on the upper fan surface.

Younger terraces intermediate in elevation between the high terrace and the active wash are preserved as a limited number of scattered exposures within the main arroyo. Clasts with very thin silica rinds were collected from the calcite-rich soils at two of these terraces between 3 and 5 m above the present channel bottom. Resulting $^{230}Th/U$ ages cluster between 27 and 31 ka for the more-northerly site at a slightly higher elevation relative to the southerly site, which has slightly younger $^{230}Th/U$ ages between about 21 and 25 ka. An older age of 35.7 ka from a clast rind at this same site has a suspiciously high initial $^{234}U/^{238}U$ activity ratio of 2.58. However, U-loss of the type described above is not responsible for the difference. Regardless of this discrepancy, dates from the inset terraces indicate that much of the 10 to 30 m of incision of the high terrace had occurred by about 30 ka.

In order to explain the pattern of aggradation of the high terrace followed by its incision, stream dynamics must have varied dramatically over the last 100 ka. Aggradation will occur when abundant sediment is supplied to the channel, but insufficient water is available to transport the material away. In contrast, incision is favored when sediment supply is low, but water abundance and stream competence are high. In the case of Fortymile Wash, aggradation of the upper fan surface occurred during the interglacial period between the last and penultimate pluvial episodes. At the same time that discharge sites became active in this region (30 to 60 ka), incision became the dominant channel response along the upper portions of Fortymile Wash. Evidence of cyclic, climate-linked filling and eroding of the Fortymile arroyo may exist in the older deposits of the high terrace. The first buried calcrete at at least two sites appears to predate the penultimate maximum pluvial (OI Stage 6 between about 150 and 130 ka) with $^{230}Th/U$ and model $^{234}U/^{238}U$ ages between about 160 and 200 ka. In addition, the aggradation process has probably been reinitiated in the early Holocene as evidenced by 9 to 6 ka deposits just below the active channel elevation in a quarry along Highway 95 (Fig. 17b).

The periods of incision between about 60 and 30 ka and again after about 20 until about 10 ka correlate closely with episodes of higher mean annual precipitation associated with the last pluvial cycle (Forester et al., 1996). This correlation, in addition to the style of fluvial processes, suggests that Fortymile Wash supported sustained flow, either seasonal or perennial, potentially over several tens of thousands of years. It is likely that this water budget would have created a focused zone of recharge to the saturated zone that may have caused gradients beneath Yucca Mountain to change direction to a west-dipping potentiometric surface. If so, Crater Flat, along with the Fortymile Wash system should be considered as potential down-gradient areas for nuclide release and transport in the saturated zone.

3. Summary of Interpretations

3.1 Stratigraphic framework

Stratigraphy varies considerably within individual deposits reflecting the variety of environments surrounding points or areas of ground water discharge. Although shallow, localized ponds may have existed, no evidence is present for a widespread lacustrine environment occupying the Amargosa Desert basin (i.e., Lake Amargosa; Swadley and Carr, 1987) that would have resulted in more-or-less uniform stratigraphy at all three different discharge areas (Crater Flat, Indian Pass and State Line). All deposits share a similarity in gross form including:

1) a dominance of clay to fine-sand particle size with little or no intercalated alluvial deposits
2) coarse to massive bedding structures
3) variable amounts of cementation consisting primarily of calcite with lesser silica and possibly halides or gypsum
4) scattered occurrences of plant and animal fossils or trace fossils.

These features are also useful in discriminating between discharge deposits and those of Tertiary lacustrine origin.

In spite of their lithologic similarities, discharge deposits do not have a stratigraphy that can be correlated throughout the Amargosa Desert area. Some of the observed stratigraphic variations are apparent in the measured sections shown in Figure 18. For instance, the Lathrop Wells Diatomite is the only deposit containing a thick diatomaceous horizon although diatoms are present in most all of the other deposits. The Amargosa River snail site is the only known site where 5 m of greenish brown silt deposits are largely devoid of carbonate-rich horizons. In contrast, deposits at the southern end of Crater Flat appear to have a higher proportion of carbonate horizons relative to most of the other deposits. These variations preclude establishing a region-wide

stratigraphic framework based on lithology or other physical macroscopic basis. Stable isotopes show a remarkable degree of homogeneity within many of the stratigraphic sections spanning the last two pluvial cycles at a single site as well as between sites (Fig. 6). Some variations in $\delta^{18}O$ and $\delta^{13}C$ are observed, but do not appear to correlate between sections. Other isotopic data sets (Sr and U) are either incomplete, lack high precision (e.g., large uncertainties in calculated initial $^{234}U/^{238}U$ activity ratios from ^{232}Th-rich samples) or show very large variations between sites related to source water variations (e.g., $\delta^{87}Sr$) to be of use for establishing a widely applicable stratigraphic framework. Instead, age determinations must be used to provide the stratigraphic framework for discharge activity that can then be related to other climate-dependent attributes.

3.2 Age of Discharge Activity

Age data, in the form of U-series disequilibrium, thermoluminescence or radiocarbon, are available for all sites shown in Figure 18. Dates obtained by the three independent methods are typically consistent with internal stratigraphy and are generally concordant where applied to materials from the same horizons. The geochronological data often do not precisely resolve millennia-scale events because of sample availability or analytical behavior. However, they provide a general framework of saturated-zone hydrologic responses that can be related to climate variations determined on a regional basis from other surface records.

The latest episode of discharge activity in the northern Amargosa Desert was between about 14 and 20 ka. A few samples collected from surface lag may extend to slightly younger ages (10 to 13 ka) at these sites, but they are from plant petrifactions that may have been tapping a water source that had already subsided below ground surface. All nodular carbonate samples and most all petrifactions and fossil shells have minimum ages of 14 to 15 ka in this area. This episode resulted in deposits typically less than a meter in thickness; however the amount of material stripped away in the 10 to 15 ka since activity ceased is unknown. In contrast, deposits at the Amargosa River snail site in the State Line area extend to slightly younger ages of 9 to 12 ka. In this case, more than 5 m of uniformly fine-grained deposits may have resulted from this cycle of activity. Evidence of discharge activity as young as 15 to 20 ka at the top of the State Line high terrace or Scranton well has not been identified.

The next cluster of dates corresponds to ages between about 30 to 60 ka. Materials with these ages are present at all sites except for the Crater Flat Wash and Amargosa River snail site where materials lower in the sections have not been analyzed. At most sites, sediment is present between horizons with dates less than 20 and greater than 30 so that it is unclear whether there is a depositional hiatus during the interval between 20 and 30 ka. Lithologic breaks between these horizons at LWD, CFD Pit 1, and IPD Station 1 as well as the lack of 20 to 30 ka dates suggest that a cessation of discharge is likely during this interval. Substantial environmental or hydrodynamic differences between the 60 to 30 ka and 20 to 15 ka episodes of activity caused the resulting deposits to change substantially. The lack of 10 to 20 ka deposits on the SLD high terrace may indicate that water table elevations did not attain their previous maximum heights during the latest high stand. In all measured sections, deposits of the 30 to 60 ka cycle are thicker than the latest deposits. This may be due to preferential erosion of the last cycle of deposits.

Several of the sites record discharge activity at about 90 ka extending throughout the penultimate pluvial cycle to about 180 or 190 ka. No geochronological evidence for distinct hiatuses during this period have been recognized; however, dates in most cases are poorly resolved. These older materials (green sand unit) have widespread exposure at the Lathrop Wells Diatomite, in arroyo walls at Mesquite Wash and in the Scranton well. However they remain largely unexposed at other sites.

3.3 Environmental and ecological conditions

Paleontological data indicate that environments around discharge sites varied laterally as well as through time and included seeps, flowing springs, and spring-supported standing water (pools, wetlands). The ostracode, mollusc and diatom species provide the basis for paleoenvironmental reconstruction at discharge sites by comparing fossil assemblages with the known environments of living examples of the same genera and species. The following discussion is summarized from Paces and others (1996).

Fossil assemblages indicate that ground water seeps were common. These environments have low levels of ground-water discharge, ranging from highly ephemeral to permanent, and involved only minor

surface water flow. Water temperature and hydrochemistry vary seasonally with warmer, higher salinity (derived through evaporative concentration) waters common during summer months. Seeps probably supported dense stands of emergents (cattails, bulrush), grasses or other vegetation. Many of the ostracode species found in seeps are tolerant of wide ranges in temperature, total dissolved solids, and major-dissolved ions. The absence of species that are less tolerant of environmental extremes supports interpretation of these deposits as seeps. Ground water often resides just below the surface at ephemeral seeps or wet-ground environments supporting emergent and other phreatophitic vegetation. Although these environments may or may not support ostracode populations, they often do support other fauna including terrestrial and semi-aquatic (air breathing) molluscs. Even under dry conditions, snails can subsist in small, persistent pools of water and in the humid microenvironments present within the vegetation.

Fossil evidence for flowing springs is also present. These environments are characterized by continuous ground-water discharge sufficient to form small streamlets that are commonly bordered by hydrophilic vegetation. Temperature and chemistry of water in streamlet varies inversely with discharge flux and may show wide seasonal variations for low-discharge springs. Ostracodes are usually common in flowing springs including species characteristic of that environment. Species from aquatic environments associated with flowing springs (aquifer-, wetland-, or stream-taxa) may also be common in flowing springs. Associated mollusc assemblages will tend to have more aquatic (air and gill breathers) and fewer terrestrial species than in seepage environments.

Spring supported pools and marshes are also documented by fossil evidence. The 2-m-thick diatom bed at the Lathrop Wells Diatomite deposit was most likely an open water environment, as were the silty deposits along the Amargosa River north of Franklin Well. These environments undoubtedly varied in size, from small pools a few meters in diameter to shallow ponds or lakes hundreds of meters in diameter. Evidence for the nature of these habitats is based not only on the fossil assemblages and the lateral distribution of wetland sediments, but also on modern analogs such as the wetlands at Ash Meadows and in Pahranagat and Ruby Marsh Valleys. Flow through these environments is typically minimal with standing water being common in the larger water bodies. These environments can be variously perennial or ephemeral.

3.4 Source of water

3.4.1 Physical Evidence: Discharge occurred synchronously at multiple sites distributed widely throughout the Amargosa Desert. In addition these sites occur within a restricted zone of elevation that decreases southward in the same sense as the underlying potentiometric surface. The lateral extents of these deposits also show a positive correlation with depth to the present-day water table. Deposits in the Crater Flat area where the depth to water is 80 to 100 m are small relative to the extensive deposits in the State Line area where depth to water is no more than several tens of meters. Although some local controls such as subsurface structural features or impingement of two fluvial systems are probably responsible for restricting locations of discharge areas, physical features provide evidence that water sources are connected to regional rather than local sources.

3.4.2 Water Temperatures: Diatoms from LWD and SLD (Mesquite Wash) suggest warm spring discharge of high-silica, alkaline-enriched water that was associated, at least in part, with the volcanic aquifer. The composition of volcanic aquifer water is commonly characterized by waters enriched in $NaCO_3$ and dissolved SiO_2 and is fundamentally different than Ash Meadows spring water which reflects the carbonate aquifer that is calcium-enriched. Diatoms from the auger hole at CFW, seems to reflect the same Na and Si-alk-enriched composition as the Lathrop Wells site according to proportional compositions reported in Carruth (1996).

The diatom flora of the Lathrop Wells deposits and at Mesquite Wash in the State Line area suggests, by analogy, thermal spring discharge. Thermal springs along the Firehole River and aquatic habitats down-stream from geysers in Yellowstone National Park are characterized by the same diatoms that occur in paleo-discharge sites near Yucca Mountain. Nevertheless, it is probable that local orifice water temperatures did not significantly exceed 30°C or if so, that the diatoms lived in cooler parts of the discharge system away from hot orifice temperatures. Indeed, at the State Line Mesquite Wash site, thermophilic diatoms such as Achnanthes thermalis are found associated with diatom taxa such as Cymbella falasiensis, C. hybrida, Pinnularia lagerstedtii, Caloneis tenuis, and Nitzschia alpina, that characterize (but are not restricted to) cold, alpine

sites in Europe and the western United States. This diatom assemblage undoubtedly represents a mixture of species from separate micro-habitats of varying ecological and environmental conditions. A consistent environmental model for this diatom assemblage would involve a thermal discharge site in a cold, wet climate. A permissible paleontological and geo-environmental correlation of the State Line deposits to the acceptably dated Lathrop Wells deposits would suggest active thermal discharge occurred during both the last and penultimate glacial period when such climatic conditions persisted. Regional ground waters often show elevated temperatures between 30 and 35° C as well as at least some restricted thermal waters in the Beatty area. If the diatom data are indicative of warmer temperatures, water must be discharging from regional rather than perched aquifers. Future research should involve biotic and paleontologic collections from active spring sites to better associate water chemistry and water sources with biological composition of ostracodes and diatoms. A minimal amount of fieldwork from selected spring sites would substantially add to the value of paleontological analyses from SLD and LWD deposits.

In contrast, temperatures estimated from $\delta^{18}O$ suggest discharge was cooler than the temperatures implied by diatom assemblages. Springs discharging from deep (warmer) carbonate-rich Paleozoic marine sedimentary rock aquifers typically contain significant concentrations of both bicarbonate and calcium and will deposit calcite veins within fracture conduits as well as carbonate tufa at the surface. Calcite samples from these sites define a calcite end member with relatively high $\delta^{13}C$ values (0 ± 2‰), and low $\delta^{18}O$ values (14 ± 1‰) (carbonate springs field on Figure 5). The high $\delta^{13}C$ is characteristic of aquifers hosted by marine carbonate rocks, whereas the lower $\delta^{18}O$ values reflect warmer discharge temperatures. Modern discharge temperatures at Grapevine and Nevares Springs in Death Valley or Devils Hole in Ash Meadows range from about 25 to 36°C. Calcite formed at these temperatures has $\delta^{18}O$ of 14±1‰ and is in isotopic equilibrium with waters of -15 to -11‰. Modern ground waters of the region have $\delta^{18}O$ of -14 to -12‰ (e.g., Benson and McKinley, 1985; Claassen, 1985; White and Chuma, 1987). The wider range of values derived from travertine deposits probably reflects long term, climate-induced variability in the $\delta^{18}O$ of meteoric waters, with lower $\delta^{18}O$ during the glacial climes.

Unlike the warm, travertine-depositing springs, the Amargosa discharge deposits typically contain carbonate only as local cements within clastic units, isolated lenses or calcified plants and calcareous invertebrate microfossils. The lowest carbonate $\delta^{18}O$ values from these deposits cluster around 19±1‰. Those materials represent calcite deposited from water least likely to have been affected by evaporative ^{18}O-enrichment or diagenesis. Using the range of -15 to -11‰ for equilibrium between discharging water and calcite, carbonate $\delta^{18}O$ values from Amargosa discharge deposits indicate temperatures ranging from <0°C (clearly unreasonable) to about 16°C. These temperatures indicate that the deposits likely formed from shallower, cooler aquifers than those discharging from the deep, carbonate aquifer. If the 19±1‰ carbonates formed from water discharging at 30°C as suggested by diatom assemblages, water compositions in equilibrium with calcite would have $\delta^{18}O$ between -9 and -7‰. These types of $\delta^{18}O$ values are anomalous compared to modern meteoric recharge occurring under the present hot, semi-arid climate and even more incongruent with recharge occurring during cooler and wetter pluvial climates when the deposits were formed.

Resolution of the conflicting temperature indicators may involve unrecognized evaporation of water prior to calcite precipitation, such that the calcite deposited in orifice environments would have lower $\delta^{18}O$. This possibility seems unlikely due to the large number of analyses, including fossil shells, from widely dispersed localities and paleo environments with uniform minimum values of 19 ± 1 ‰. Conversely, although the observed diatom assemblages are commonly found living in warm spring environments, their lower temperature tolerances have not been strictly determined. It may be possible that if dissolved silica contents are sufficiently high, thermophilic species may be able to survive in cold (15 to 20° C) spring environments.

3.4.3 Paleontological Evidence: Diatom assemblages within the CFW deposits reflect a mixture of both volcanic and carbonate-rich aquifer systems, the latter perhaps moving south from the Crater Flat region where calcium, magnesiun bicarbonate ground water had been documented (Thompson and Chappell, 1984). The generally poorer preservation of diatoms

at the CFW locality could imply a smaller volume of silica-rich water discharging at this site relative to those at LWD or SLD Mesquite Wash. Similarly, the near complete absence of diatoms at the CFD locality may indicate the predominance of calcium, magnesiun bicarbonate water chemistries affecting discharge at that site and dissolving diatoms in the process.

3.4.4 Tracer Isotopes: Tracer isotopes, including $\delta^{87}Sr$, $\delta^{13}C$, and initial $^{234}U/^{238}U$ preclude a surface origin and generally do not support perched-zone origins (Paces et al., 1996). Data indicate that discharging waters were mixtures of "typical" regional ground waters (i.e., carbonate and volcanic aquifers). Data collected in FY97 are consistent with previously obtained data, summarized in Tables 8, and are given in the form of a matrix of possible water sources in Table 9. Interpretations based on these data are not consistent with a single aquifer type unlike the uniform, long-term records at Devils Hole (Winograd et al., 1992; Ludwig et al., 1992). The reason for this is probably linked to the nature of the shallow aquifer system occupying alluvial fill basins as well as the highly variable environments associated with discharge sites that provide further opportunities for mixing with atmospheric, run off and pedogenic components. Mixed sediments within alluvial aquifers will impart varying isotopic signatures to the water which will then becomes a hydrochemical hybrid between a purely "Paleozoic" or "volcanic" aquifer. For instance, the ubiquitous presence of diatoms along with elevated $\delta^{87}Sr$ and $^{234}U/^{238}U$ compositions are indicative of volcanic aquifer source; however, $\delta^{13}C$ values indicate probable reaction with Paleozoic rocks within the alluvial aquifers. Similarly, elevated $\delta^{87}Sr$ in the deposits of the State Line area indicate addition of radiogenic Sr commonly not present within the bulk of the Tertiary volcanic rocks. A critical test of a saturated-zone source for the discharge deposits would be to determine if present-day SZ waters at depth have similar compositions. Unfortunately the shallow wells intended to sample the aquifers beneath the discharge sites have not been drilled.

3.5 Frequency and rapidity of water table fluctuations

Although complicated by the factors outlined above, deposits most certainly represent discharge from the regional aquifer. Present-day depths to water vary from between 80 to 100 m in the Crater Flat vicinity to only 10 to 20 meters in the State Line area. Therefore, the discharge deposits document periods of time when the water table responded to the higher effective moisture available in recharge areas during pluvial episodes. The absence of similar deposits at higher elevations suggests that these deposits represent maximum water table heights. Similar estimates of maximum water table elevations under Yucca Mountain have been made on the basis of the distribution of zeolitization in tuffs (Levy, 1991) and from hydrologic models using a 1500 percent increase in recharge (double precipitation) relative to modern-day (Czarnecki, 1985).

The rapidity of water table response to changes in recharge can only be approximated using current information. Not only are the ages of depositional events poorly resolved (typically several thousand years at best), but also the record of recharge is also only generally known by extrapolation from various surface climate-proxy records. Ages from discharge deposits tend to cluster during periods of time that have been recognized elsewhere as records of higher mean annual precipitation and cooler conditions (described below). In many cases, these records are remarkably similar; whether they represent the response of a surface process or of ground water flow paths that vary greatly in length. The age similarities between timing of discharge at the Amargosa deposits and these other records suggests that response did not require long periods of time (tens of thousands of years) to adjust to new climate conditions. In addition, climate change may have been gradual over several millennia such that water levels adjusted simultaneously. If climate shifts were dramatically abrupt, water table elevation changes probably occurred on a scale of less than several millennia.

Results from the current study indicates that 100 m water table fluctuations have occurred repeatedly (at least twice) during the last two glacial cycles. If these recharge conditions recur in the future due to similar orbital configurations, it is likely that discharge activity will be renewed. These conclusions contrast sharply with those reached in early studies that attributed changes in water table height to slower, geologic processes (Winograd and Szabo, 1988). A number of travertine veins originally associated with saturated zone deposition were found exposed at the surface at elevations more than 10 to 50 m above present-day water table (Winograd and Doty, 1980). Veins above modern water levels by at least 11 m

were dated at greater than 500 ka (Winograd et al., 1985; Winograd and Szabo, 1988). Furthermore, water in fluid inclusions within these calcites shows a pattern of unidirectional δ^2H depletion of about 40 ‰ over the last 2 million years (Winograd et al., 1985). The lower δ^2H values in more recent veins were attributed to the effects of uplift in the Sierra Nevada and Transverse Ranges since the Pliocene resulting in lowered δ^2H in the water vapor before air masses reach southern Nevada. Rates of unidirectional water table decline were also calculated from dated travertine veins at known heights above the present water table. Values based on three veins in the Ash Meadows area implied apparent decline rates of about 0.02 to 0.08 m/ka (Winograd and Szabo, 1988) whereas rates at Furnace Creek Wash were estimated as high as 0.2 to 0.6 m/ka.

Although moisture infiltrating into recharge areas in Nevada may have lower δ^2H values today relative to those during the Pliocene, episodic discharge throughout the late Pleistocene at the Amargosa sites indicates that the water table in this area is not monotonically declining. Factors not related to absolute water table elevations, such as tectonic movements, or critical assumptions about the age determinations (i.e., no recent deposition on outermost layers that would provide a mixed age much younger than the bulk of the vein) are more likely the explanation of the apparent water table declines proposed by Winograd and Szabo (1988).

3.6 Comparisons to other climate records

3.6.1 Devils Hole: Subaqueously deposited calcite at Devils Hole (about 50 ka southwest of Yucca Mountain in the Ash Meadows discharge area) contains a dated record of the $\delta^{18}O$ composition of water infiltrating into recharge areas between 600 and 60 ka (Winograd et al, 1992; Ludwig et al., 1992). The $\delta^{18}O$ isotopic variations largely reflect average winter and spring land surface temperatures (Winograd et al, 1992) and show a cyclic variation of about 3‰ Lowest $\delta^{18}O$ values correlate closely to times of maximum continental glaciation over the last 450 ka. These data show that climate in southern Nevada responded to global climate variations and that ground water compositions faithfully preserve climate signals inherited from recharge areas. Cold climate episodes recur on about 100 ka cycles and are followed by a rapid return to warmer conditions with gradually cooling conditions until the next cold interval. Although these signals clearly indicate climate change, they do not directly equate to moisture available at recharge areas.

Carbon isotopes show a similar but reversed pattern of variation in the same Devils Hole record (Coplen et al., 1994). Thus, $\delta^{13}C$ preserves the same climate signal as $\delta^{18}O$; however, the cause of the observed variation is not as clear. A likely explanation relates $\delta^{13}C$ variation to the extent and density of vegetation in recharge areas. Colder climates associated pluvial periods most likely resulted in alpine and sub-alpine vegetation instead of sub-alpine and montane vegetation, respectively, that occurred at the same elevations during interglacial periods. Like $\delta^{18}O$, $\delta^{13}C$ records climate change; however, $\delta^{13}C$ is not clearly related to effective moisture in recharge areas.

In addition to records of thermal variation, Devils Hole also preserves a history of water table fluctuation over the last 100 ka (Szabo et al., 1994). A 9 m high subterranean, air-filled chamber named Browns Room has a variety of calcite deposits coating walls at various heights. Folia deposits (horizontal, terrace-like structures) form on overhanging walls near mean water levels. Therefore, these deposits record the height of the water table at various different times in the past. Age determinations indicate water levels up to 9 m higher than modern water levels between about 45 and 18 ka (Szabo et al., 1994). Water levels may have been lower than this (less than 6 m) between about 37 to 30 ka. By about 10 ka, water levels had lowered to only about 4 m above present and continued to decline systematically throughout the Holocene. Data provide less detail for water levels older than about 45 ka, but appear to record a water stand at least 5 m higher than modern between 45 and 110 ka. These data clearly document higher water levels in a major aquifer that are generally coincident with formation of the Amargosa discharge deposits.

3.6.2 Owens Lake: Core from Owens Lake provides a record of freshwater and saline conditions related to the amount of influx from the Owens River system draining the Sierra Mountains to the west with lesser contributions from the Inyo and White Mountains to the east. Both fossil diatoms and ostracodes in the Owens Lake long core reflect water chemistry that can be translated into a progression of climate-induced hydrochemical environments (Forester et al., 1996). The dominant taxa change within the core and document conditions varying

from fresh, calcium bicarbonate-rich water indicative of cool, wet climates to shallow, warm, sodium bicarbonate-rich water indicating conditions of reduced mountain runoff, increased evaporation, and greater relative input of local spring discharge. Paleontological evidence indicates that the lake has been dominated by saline conditions during the Holocene interglacial period. Freshwater conditions prevailed between about 10 and 50 ka representing the last pluvial cycle. The period between about 50 and 90 to 100 ka was again dominated by saline conditions though freshwater taxa are present at times between 50 and 70 ka. The lake returned to dominantly freshwater conditions for much of the penultimate pluvial episode between about 90 to 180 ka. Oxygen Isotope Stage 5e interglacial may be represented between about 110 and 120 by the presence of saline taxa; however, freshwater species are nevertheless abundant in the same intervals. Percentages of freshwater taxa drop off to nearly zero between 170 and 200 ka at the same time the saline species increase sporadically between this interval indicating a return to interglacial conditions.

The climate/hydrologic relations observed in the Owens Lake core generally reflect the same patterns of higher water table elevations in the Amargosa discharge deposits throughout the last two glacial cycles. Both records appear to contain evidence for wetter conditions between about 15 and 60 ka, possibily including evidence of a drier period around 30 ka. Both records also show evidence of dry conditions between 60 and 90 ka as well as some evidence that wetter episodes existed during Oxygen Isotope Stage 5 (between 90 and 130 ka) subsequent to the penultimate glacial maximum (OI Stage 6).

3.6.3 Corn Creek: Discharge deposits flank the Spring Mountains in both Pahrump and Las Vegas Valleys (Quade et al., 1995). These deposits have been interpreted as spring, marsh, seep and wet-ground environments associated with shallow groundwater traveling through alluvial fans from recharge areas in the high Spring and Sheep Mountains. The stratigraphy for these deposits has been established and dated using radiocarbon on organic materials and carbonate from mollusc shells (Quade, 1986; Quade et al., 1995, Forester et al., 1996; Brennan and Quade, 1997).

Studies have focused on the younger portions of these deposits either because of lack of deeper exposure, or age limits of the ^{14}C chronometer. Oldest units (stratigraphic unit B), where present, have radiocarbon ages from mollusc shells between about 35 and 42 ka. The possibility of small amounts (less than one to two percent) of recrystallization or contamination with modern carbon will provide enough ^{14}C in an otherwise old (>50 ka), ^{14}C-free shell to give ages in this range. Therefore, these deposits could either be related to earliest stages of the ultimate pluvial event, or to the penultimate cycle over 100 k.y. At Corn Creek (Las Vegas Valley), radiocarbon ages in the overlying unit D are bimodal with ages between 34 and 36 ka for the lower portions (D_1) and 18 to 19 ka for upper portions (D_2). The apparent disconformity between these units presumably represents a hiatus caused by non-deposition. At the same locality, the overlying unit E has conventional radiocarbon ages of around 12 to 13 ka, which have calendar dates of several thousand years older. Youngest materials from these deposits have radiocarbon ages between 8 and 10 ka.

These deposits discharging from alluvial fans flanking nearby highlands overlap ages from the youngest units in the Amargosa Desert vicinity almost exactly. In particular both data sets tend to lack materials dated in the 20 to 30 ka range. With the exception of the Amargosa River snail site, deposits in the Amargosa Desert typically lack the youngest episode of discharge. This could be related to the more-local recharge source in the valleys surrounding the Spring and Sheep Mountains relative to the Amargosa deposits that are dependent on more remote recharge sources. In spite of differences in proximal and distal recharge sources, both sets of deposits record water table fluctuations occurring at nearly the same times. This provides evidence that the saturated zone readjusts to climate shifts without significant lag time.

3.6.4 Fortymile Wash: As described above, the surface response to climate change manifested itself by readjusting fluvial processes. High terrace deposits were formed between 50 and 100 ka followed by major incision of more than 20 m over the next 20 to 30 k.y. Intermediate terrace levels formed between 20 and 30 k.y. suggest a suspension in erosion; however, it resumed between about 20 and 10 ka. These ages indicative of greater amounts of available surface water correspond remarkably well to discharge activity in the Amargosa deposits, suggesting that water table response to climate change was rapid.

4. Conclusions

Regional saturated zone ground water responds to climate-induced changes in effective moisture, infiltration and recharge.

Discharge sites down-gradient from the potential repository block were active intermittently throughout the last 200 ka. Ages cluster between 90 to 180 ka, 30 to 60 ka, and 14 to 20 ka, with resolution increasing in the younger materials.

Most recent activity ceased around 12-16 ka at higher elevations on the north side of the Amargosa Desert and slightly later (9-10 ka) at lower elevation on south side of valley.

Spring activity is synchronous at widely distributed deposits throughout the Amargosa Valley and adjoining valleys. Elevation of the deposits decreases southward in a manner consistent with the regional ground-water gradient.

Paleontology indicates variety of spring-fed wet-ground, seep, marsh, flowing spring and open-pool environments. Diatoms indicate may indicate freely flowing, "warm" (<30°C), low-salinity, alkaline discharge at the LWD site.

Oxygen isotopes indicate that water temperatures at paleo spring sites were cooler than present-day springs discharging from the regional carbonate aquifer or that recharge occurred at lower elevations in the past.

U, Sr, and carbon isotope data indicate discharge from a regional aquifer rather than from surface or perched sources. Isotope as well as ostracode and diatom data suggest a mixture of "pure aquifer" end-members that is most readily accounted for by discharge from a shallow alluvial aquifer with mixed sedimentary fill. Hydrochemical samples from beneath most sites that would directly address a saturated-zone source are lacking.

Saturated zone discharge requires that the regional water table was elevated up to 100 m (± 20 m) above its present-day surface in southern Crater Flat.

Water table fluctuations occurred repeatedly at times that correlate closely to wetter portions of last two pluvial cycles. Records at Amargosa discharge sites are consistent with the timing of events indicative of greater mean annual precipitation and lesser mean annual temperature at Devils Hole, Owens Lake, Corn Creek (i.e., Las Vegas and Pahrump Valley discharge deposits), and Fortymile Wash.

Evidence for substantial lag times between the onset of cooler, wetter pluvial conditions and water table high-stands based on surface records is absent indicating that water tables respond to changes in climate-induced recharge within several millennia.

Discharge may have been active for more than half of the last 200 ka. Therefore, water table elevations higher than present day may be the norm for the late Quaternary.

A tectonic (Sierra Nevada, Transverse Range uplift combined with lowering of Death Valley baselevel) model of unidirectional decline in water table elevations is unsupported by these studies of the Yucca Mountain system.

Higher water table elevations are likely to occur in the future if climate is driven by cyclic orbital parameters.

Localized recharge in Fortymile Wash during pluvial episodes affects the underlying water table to a greater degree and most likely changes the potentiometric surface gradients from generally east-dipping to west-dipping.

Natural lowering of water table elevations of at least several meters may have occurred in historical times (dry hand-dug wells). Transient rather than steady-state hydrologic flow models are necessary to effectively model future saturated zone conditions.

Past discharge volumes are unknown, but estimates are possible based on present-day discharges, lateral extents and sedimentation rates at Ash Meadows and Franklin Lake Playa.

REFERENCES

Anderson, R.F., Bacon, M.P., and Brewer, P.G., 1982, Elevated concentrations of actinides in Mono Lake. Science, vol. 216, p. 514-16.

Benson, L.V., and McKinley, P.W., 1985, Chemical composition of ground water in the Yucca Mountain Area, Nevada, 1971-84: U.S. Geological Survey Open-File Report 85-484, 10 p.

Brennan, R., and Quade, J., 1997, Reliable late-Pleistocene stratigraphic ages and shorter

groundwater travel times from ^{14}C in fossil snails from the southern Great Basin. Quaternary Research, vol. 47, p. 329-336.

Carruth, R.L., 1996, Hydrogeology of the Quitobaquito Springs and the Abra Plain area, Organ Pipe Cactus National Monument, Arizona and Sonora Mexico: U.S. Geological Survey Water Resources Investigation Report 95-4295, 23 p.

Claassen, H.D., 1985, Sources and mechanisms of recharge for ground water in the west-central Amargosa Desert, Nevada - A geochemical interpretation: U.S. Geological Survey Professional Paper 712-F, 31 p.

Coplen, T.B., Winograd, I.J., Landwehr, J.M., and Riggs, A.C., 1994, 500,000-year stable carbon isotopic record from Devils Hole, Nevada: Science, v. 263, p. 361-365.

Czarnecki, J.,1985, Simulated effects of increased recharge on the ground-water flow system of Yucca Mountain and vicinity, Nevada-California. U.S. Geological Survey Water Resources Investigation Report 84-4344, 33 p.

Ervin, E.M., Luckey R.R., and Burkhardt, D.J., 1993, Summary of revised potentiometric-surface map for Yucca Mountain and vicinity, Nevada. Proceedings, Fourth International Conference of High Level Radioactive Waste Management, Las Vegas, NV, April 26-30, 1993, American Nuclear Society, La Grange Park, IL., p. 1554-1558.

Forester R.M., Bradbury, J.P., Carter, C., Elvidge, A., Hemphill, M., Lundstrom, S.C., Mahan, S.A., Marshall, B.D., Neymark, L.A., Paces, J.B., Sharpe, S., Whelan, J.F., and Wigand, P., 1996, The climatic and hydrologic history of southern Nevada during the Late Quaternary: U.S. Geological Survey Milestone report 3GCA102M to DOE-YMPSCO.

Hay, R.L., Pexton, R.E., Teague, T.T., and Kyser, T.K., 1986, Spring-related carbonate rocks, Mg clays, and associated minerals in Pliocene deposits of the Amargosa Desert, Nevada and California. Geological Society of America Bulletin, v. 97, p. 1488-1503.

Imbrie, J, Hay, J., Martinson, D.G., McIntyre, A., Mix, A.C., Morley, J.J., Pisias, N.G., Press, W.L., and Shackleton, N.J., 1984, The orbital theory of pleistocene climate: Support from a revised chronology of the marine 18O record: In Milankovich and Climate, Part I, A. Berger, J. Imbrie, J. Hay, S. Gupka, B. Saltzman (Eds.), Reidel, Boston, MA., p. 269-305.

LaFlamme, B.D., and Murray, J.W., 1987, Solid/solution interaction: the effect of carbonate alkalinity on adsorbed thorium. Geochimica et Cosmochimia Acta, vol. 51, p. 243-250.

Levy, S.S. (1991), Mineralogic alteration history and paleohydrology at Yucca Mountain, Nevada. High-Level radioactive Waste Management Proceedings of the Second International Conference, p. 477.

Ludwig, K.R., Simmons, K.R., Szabo, B.J., Winograd, I.J., Landwehr, J.M., Riggs, A.C., and Hoffman, R.J., 1992, Mass-spectrometeric 230Th-234U-238U dating of the Devils Hole calcite vein: Science v. 258, p. 284-287.

Paces, J.B., Forester, R.M., Whelan, J.F., Mahan, S.A., Bradbury, J.P., Quade, J., Neymark, L.A., and Kwak, L., 1996, Synthesis of ground-water discharge deposits near Yucca Mountain: U.S. Geological Survey Milestone Report 3GQH671M to DOE-YMPSCO, 75 p.

Paces J.B., 1995, FY1995 studies of paleodischarge deposits: Milestone Report 3GQH520M to DOE-YMPSCO, 27 p.

Peterman Z.E., and Stuckless, J.S. (1993) Isotopic evidence of complex ground-water flow at Yucca Mountain, Nevada, USA: *in* Conference on High-Level Radioactive Waste Management, 4th, Las Vegas, NV, 1993, Proceedings, American Society of Civil Engineers, p. 1559-1566.

Peterman, Z.E., Widmann, B.L., Marshall, B.D., Aleinikoff, J.N., Futa, K., and Mahan, S.A. (1994) Isotopic tracers of gold deposition in Paleozoic limestones, southern Nevada: *in* Conference on High-Level Radioactive Waste Management, 5th, Las Vegas, NV, Proceedings, American Society of Civil Engineers, p. 1316-1323.

Quade, J., Mifflin, M.D., Pratt, W.L., McCoy, W., and Burckle, L., 1995, Spring deposits and water table levels in the southern Great Basin

during the late Quaternary: Geological Society of America Bulletin, v. 107, p. 213-230.

Quade, J., 1986, Late Quaternary environmental changes in the upper Las Vegas Valley. Quaternary Research, v. 26, p. 340-357.

Simpson, H.J., Trier, R.M., Toggweiler, J.R., Mathiew, G. Deck, B.L., and Olsen C.R., 1982, Radionuclides in Mono Lake California. Science, vol. 216, p. 512-514.

Swadley, W.C., and Carr, W.J. (1987) Geologic map of the Quaternary and Tertiary deposits of the Big Dune Quadrangle, Nye County, Nevada, and Inyo County, California: U.S. Geological Survey Miscellaneous Series Map, I-1767.

Szabo, B.J., Kolesar, P.T., Riggs A.C., Winograd, I.J., and Ludwig K.R., 1994, Paleoclimatic inferences from a 120,000-yr calcite record of water-table fluctutation in Browns Room of Devils Hole, Nevada: Quaternary Research, v. 41, p. 59-69.

Thompson, T.H. and Chappell, R., 1984, Maps showing distribution of dissolved solids and dominant chemical type in ground water, Basin and Range Province, Nevada: Water-Resources Investigations Report 84-4119-C.

White, A.T., and Chuma, N.J., 1987, Carbon and isotope mass balance models of Oasis Valley-Fortymile Canyon groundwater basin, southern Nevada: Water Resources Research, v. 23, p. 571-582.

Winograd, I.J., and Doty, G.C., 1980, Paleohydrology of the southern Great Basin with special reference to water table fluctuations beneath the Nevada Test Site during the late(?) Pleistocene: U.S. Geological Survey Open-File Report 80-569, 91 p.

Winograd, I.J., and Szabo, B.J., 1988; Water-table decline in the south-central Great Basin during the Quaternary: Implications for toxic waste disposal: in Carr, M.D. and Yount, J.C., eds., Geologic and Hydrologic Investigations, Yucca Mountain, Nevada, U.S. Geological Survey Bulletin 1790, p. 147-152.

Winograd, I.J, Szabo, B.J., Coplen T.B., Riggs, A.C., and Kolesar, P.T., 1985, Two-million-year record of deuterium depletion in Great Basin ground waters: Science, v. 227, p. 519-522.

Winograd, I.J., Coplen, T.B., Landwehr, J.M., Riggs, A.C., Ludwig, K.R., Szabo, B.J., Kolesar, P.T., and Revesz, K.M., 1992, Continuous 500,000-year climate record from vein calcite in Devils Hole, Nevada: Science, vol. 258, p. 255-260.

FIGURE CAPTIONS

Figure 1: Location map showing Amargosa discharge deposits.

Figure 2: Topographic map of the Franklin Well and Scranton Well area. Shaded areas represent mesquite thickets along the Amargosa River bottom.

Figure 3: Generalized sections showing sample locations and corresponding ages for State Line deposits at Mesquite Wash.

Figure 4: U-series evolution diagram showing U and Th isotopic results for data from State Line Deposits near Franklin Well.

Figure 5: Plot of new $\delta^{13}C$ and $\delta^{18}O$ data of carbonates from stratigraphic sequences collected at the State Line Deposits including Mesquite Wash and the High Terrace samples (filled squares), Amargosa River snail site (open circles) and Scranton Well (dark crosses). Fields defined by preexisting data from Amargosa Valley Tertiary lacustrine limestones, carbonate-aquifer tufas and travertines (Death Valley, Devils Hole), and Amargosa discharge deposits at SLD CFD, and LWD are shown for comparison.

Figure 6: Graphs of the $\delta^{13}C$ (filled squares) and $\delta^{18}O$ (filled circles) versus depth for five sections collected from Amargosa discharge deposits in FY97. Depositional ages are from Figure 18.

Figure 7: Correlation between Sr isotopic composition and inverse concentration for some carbonate-rich samples in the Mesquite Wash area of the State Line past discharge deposits. Values adjacent to symbols are d87Sr compositions given in Table 3.

Figure 8: Variations of Sr isotopic composition and concentrations with depth in the Mesquite Wash section of the State Line discharge

deposits. Data represented by open diamonds are from Paces (1995).

Figure 9: Schematic representation of snail site auger hole showing sampled intervals, ostracode assemblages and TL ages (TL-46 data from Paces et al., 1996).

Figure 10: Schematic representation of units exposed in walls of the dry Scranton Well showing sampled intervals and resulting $^{230}Th/U$ ages.

Figure 11: U-series evolution diagram showing U and Th isotopic results for data from Scranton Well.

Figure 12: Sketch of air photos showing major morphologic features of the Lathrop Wells Diatomite deposit. Light-colored, fine-grained deposits are shown as light-shaded areas. Area with platy veneer of banded dense limestone shown with darker-shading. Numbered stations are shown with circle/cross symbol.

Figure 13: U-series evolution diagram showing U and Th isotopic data for analyses from LWD.

Figure 14: Sketch of air photos showing major morphologic features of the Crater Flat Wash deposit (CFW). Light-colored, fine-grained deposits are shown as light-shaded areas. Numbered sample stations are shown with small black circles.

Figure 15: Schematic representation of CFW AUGER-1 hole showing sampled intervals and ostracode assemblages.

Figure 16: Schematic representation of continuously collected auger-bucket samples from CFD Station 5 auger hole.

Figure 17: A) General geomorphic map of the southern Nevada and Eastern California showing the Fortymile Wash drainage system along with Quaternary discharge deposits in the southern Amargosa valley. B) Upper portion of the Fortymile Wash showing sites sampled for dating. Solid lines represent active ephemeral channels. Dotted lines represent arroyo walls incised into surrounding fan surface.

Figure 18: Stratigraphic and geochronologic framework of ground water discharge deposits in the Amargosa Desert and adjoining areas. Data are generalized from this report and from Paces and others (1996). Base map as in Figure 1.

Appendix 1. Carbonate $\delta^{13}C$ and $\delta^{18}O$ values from paleo-discharge deposits in southwest Nevada.

HD #	Sample #	Locality	Depth (m)[1]	$\delta^{13}C_{PDB}$	$\delta^{18}O_{SMOW}$	Cmnts	SPC #
HD-2213 a	RC-no depth (~30)	CF Wash	0.30	-1.6	26.7	3.6m bucket augur hole - ~30cm depth	00516829
HD-2213 b	RC-70	CF Wash	0.70	-4.0	23.0	3.6m bucket augur hole - ~70cm depth	00516829
HD-2213 c	RC-100	CF Wash	1.00	-3.9	22.2	3.6m bucket augur hole - ~100cm depth	00516829
HD-2213 d	RC-NO DEPTH	CF Wash	1.30	-2.4	23.0	3.6m bucket augur hole - ~130cm depth	00516829
HD-2213 e	RC-140	CF Wash	1.40	-3.2	21.9	3.6m bucket augur hole - ~140cm depth	00516829
HD-2213 f	RC-NO DEPTH	CF Wash	1.70	-2.4	22.4	3.6m bucket augur hole - ~170cm depth	00516829
HD-2213 g	RC-195	CF Wash	1.95	-2.4	23.1	3.6m bucket augur hole - ~195cm depth	00516829
HD-2213 g	RC-195	CF Wash	1.95	-2.6	22.9	3.6m bucket augur hole - ~195cm depth	00516829
HD-2213 h	RC-no depth (230)	CF Wash	2.30	-2.9	22.1		00516829
HD-2213 j	RC-270	CF Wash	2.70	-2.3	25.0		00516829
HD-2213 n	RC-360	CF Wash	3.60	-2.7	24.4		00516829
HD-2216 a	199-5-10cm	Crater Flat	0.10	-3.5	18.6	sta. 5 at crater flat - 1.2m bucket augur hole	00516832
HD-2216 a	199-5-10cm	Crater Flat	0.10	-3.5	18.4	sta. 5 at crater flat - 1.2m bucket augur hole	00516832
HD-2216 b	199-5-25cm	Crater Flat	0.25	-3.8	18.6	sta. 5 at crater flat - 1.2m bucket augur hole	00516832
HD-2216 c	199-5-35cm	Crater Flat	0.35	-3.8	18.5	sta. 5 at crater flat - 1.2m bucket augur hole	00516832
HD-2216 d	199-5-40cm	Crater Flat	0.40	-3.9	18.6	sta. 5 at crater flat - 1.2m bucket augur hole	00516832
HD-2216 e	199-5-50cm	Crater Flat	0.50	-3.0	19.8	sta. 5 at crater flat - 1.2m bucket augur hole	00516832
HD-2216 f	199-5-57cm	Crater Flat	0.57	-1.4	22.0	sta. 5 at crater flat - 1.2m bucket augur hole	00516832
HD-2216 g	199-5-67cm	Crater Flat	0.67	-2.5	19.6	sta. 5 at crater flat - 1.2m bucket augur hole	00516832
HD-2216 h	199-5-73cm	Crater Flat	0.73	-2.9	19.9	sta. 5 at crater flat - 1.2m bucket augur hole	00516832
HD-2216 i	199-5-85	Crater Flat	0.85	-1.7	20.4	sta. 5 at crater flat - 1.2m bucket augur hole	00516832
HD-2216 j	199-5-95	Crater Flat	0.95	-1.4	20.4	sta. 5 at crater flat - 1.2m bucket augur hole	00516832
HD-2216 k	199-5-100	Crater Flat	1.00	-1.6	20.0	sta. 5 at crater flat - 1.2m bucket augur hole	00516832
HD-2216 l	199-5-110	Crater Flat	1.10	-0.4	19.2	sta. 5 at crater flat - 1.2m bucket augur hole	00516832
HD-2216 m	199-5-117	Crater Flat	1.17	-0.1	19.7	sta. 5 at crater flat - 1.2m bucket augur hole	00516832
HD-2216 n	199-5-123	Crater Flat	1.23	0.2	19.5	sta. 5 at crater flat - 1.2m bucket augur hole	00516832
HD-2207 a	10CM SLD-CORE	Franklin Wells	0.10	-2.8	22.2	sed spls taken from 5m bucket auger hole	00516832
HD-2207 b	SLD-CORE-50CM	Franklin Wells	0.50	-1.4	24.0	sed spls taken from 5m bucket auger hole	00516832
HD-2207 c	SLD-CORE 110CM	Franklin Wells	1.10	-4.0	21.3	sed spls taken from 5m bucket auger hole	00516823
HD-2207 d	SLD-CORE 180CM	Franklin Wells	1.80	-0.9	19.2	nodules -sed spls taken from 5m bucket auger	00516832
HD-2207 e	SLD-CORE 205CM	Franklin Wells	2.05	-3.5	19.8	sed spls taken from 5m bucket auger hole	00516823
HD-2207 i	SLD-CORE 400CM	Franklin Wells	4.00	-3.4	23.1	sed spls taken from 5m bucket auger hole	00516832

[1] - Depth below surface (in meters)

Appendix 1. Carbonate $\delta^{13}C$ and $\delta^{18}O$ values from paleo-discharge deposits in southwest Nevada.

HD #	Sample #	Locality	Depth (m)[1]	$\delta^{13}C_{PDB}$	$\delta^{18}O_{SMOW}$	Cmnts	SPC #
HD-2207 j	SLD-CORE 440CM	Franklin Wells	4.40	-1.9	21.3	sed spls taken from 5m bucket auger hole	00516832
HD-2207 k	SLD-CORE 460CM	Franklin Wells	4.60	-3.3	19.3	sed spls taken from 5m bucket auger hole	00516832
HD-2207 m	SLD-CORE 500CM	Franklin Wells	5.00	-2.2	22.6	sed spls taken from 5m bucket auger hole	00516832
HD-2217	120596-HTD-1	LW Diatomite		-2.3	22.3		00516833
HD-2218	120596-HTD-2	LW Diatomite		-1.7	20.2		00516834
HD-2219	120596-HTD-3	LW Diatomite		-2.1	20.3		00516834
HD-2220	120596-HTD-4	LW Diatomite		-2.2	20.4		00516836
HD-2221	120596-HTD-5	LW Diatomite		-3.0	20.7		00516837
HD-2222 b	RV-120596-JWA	Rock Valley		-0.4	23.2	lite carb	00516838
HD-2223 a	RV-120596-JWB	Rock Valley		-4.1	20.0	carb	00516839
HD-2224 a	RV-120596-JWC	Rock Valley		-0.8	21.6	carb	00516840
HD-2225 a	RV-120596-JWD	Rock Valley		-2.1	15.8	carb	00516841
HD-2208 a	Scranton 25CM	Scranton Well	0.30	-0.2	20.1	series of subspls from 6m deep hand-dug well	00516824
HD-2208 b	Scranton 50CM	Scranton Well	0.50	-1.3	19.1	series of subspls from 6m deep hand-dug well	00516824
HD-2208	Scranton 80CM	Scranton Well	0.80	-0.2	19.2	series of subspls from 6m deep hand-dug well	00516824
HD-2208	Scranton 110CM	Scranton Well	1.10	0.0	18.9	series of subspls from 6m deep hand-dug well	00516824
HD-2208	Scranton 110CM	Scranton Well	1.10	0.0	19.0	series of subspls from 6m deep hand-dug well	00516824
HD-2208 d	Scranton 150CM	Scranton Well	1.50	-1.6	19.3	series of subspls from 6m deep hand-dug well	00516824
HD-2208	Scranton 200CM	Scranton Well	2.00	-0.4	19.3	late coat - series of subspls from 6m deep	00516824
HD-2208	Scranton 200CM	Scranton Well	2.00	-1.6	18.5	matrix - series of subspls from 6m deep	00516824
HD-2208 f	Scranton 240CM	Scranton Well	2.40	-2.0	19.1	series of subspls from 6m deep hand-dug well	00516824
HD-2208 g	Scranton 275CM	Scranton Well	2.75	-1.9	20.0	series of subspls from 6m deep hand-dug well	00516824
HD-2208 h	Scranton 310CM	Scranton Well	3.10	-0.7	19.2	series of subspls from 6m deep hand-dug well	00516824
HD-2208 i	Scranton 360CM	Scranton Well	3.60	-0.4	18.7	series of subspls from 6m deep hand-dug well	00516824
HD-2208 j	Scranton 380CM	Scranton Well	3.80	-0.3	20.2	series of subspls from 6m deep hand-dug well	00516824
HD-2208 k	Scranton 400CM	Scranton Well	4.00	-0.9	18.9	series of subspls from 6m deep hand-dug well	00516824
HD-2208 n	Scranton 530CM	Scranton Well	5.30	-0.9	19.6	series of subspls from 6m deep hand-dug well	00516824
HD-2208 o	Scranton 600CM	Scranton Well	6.00	-0.9	19.3	series of subspls from 6m deep hand-dug well	00516824
HD-2186	SL-120396-JW3	Stateline-Mesq	4.50	-1.6	19.5	gm carb sand - 450cm below terrace surface	00516802
HD-2187	SL-120396-JW4	Stateline-Mesq	4.60	-1.4	19.6	gm carb sand - 460cm below terrace surface	00516803
HD-2193	SL-120396-JW9A	Stateline-Mesq	2.75	-0.5	25.0	carb nod - 275cm below terrace surface	00516809
HD-2194	SL-120396-JW10	Stateline-Mesq	2.10	0.2	26.4	fine carb sand - 210cm below terrace surface	00516810

[1] - Depth below surface (in meters)

Appendix 1. Carbonate $\delta^{13}C$ and $\delta^{18}O$ values from paleo-discharge deposits in southwest Nevada.

HD #	Sample #	Locality	Depth (m)[1]	$\delta^{13}C_{PDB}$	$\delta^{18}O_{SMOW}$	Cmnts	SPC #
HD-2194	SL-120396-JW10	Stateline-Mesq	2.10	0.5	26.8	fine carb sand - 210cm below terrace surface	00516810
HD-2195	SL-120396-JW11	Stateline-Mesq	1.80	-1.7	25.9	cream carb sand - 180cm below terrace surface	00516811
HD-2196	SL-120396-JW12	Stateline-Mesq	1.40	-0.1	27.5	cream carb - 140cm below terrace surface	00516812
HD-2197	SL-120396-JW13	Stateline-Mesq	0.00	-3.8	22.2	carb sand - lag from surface	00516813
HD-2198	120396-SLMW-1	Stateline-Mesq	5.25	-1.7	20.1	carb horiz - 525cm below terrace surface	00516814
HD-2199	120396-SLMW-2	Stateline-Mesq	4.30	-1.7	19.9	wht carb sand - 430cm below terrace surface	00516815
HD-2200	120396-SLMW-3	Stateline-Mesq	3.95	-1.6	19.5	wht carb sand - 395cm below terrace surface	00516816
HD-2200	120396-SLMW-3	Stateline-Mesq	3.95	-1.6	19.5	wht carb sand - 395 cm below terrace surface	00516816
HD-2209	120496-TEC-1	Tecopa Lake		-1.3	21.3	buff ls from within 50cm of outcrop top	00516825
HD-2211 a	TEC-120496-JW1	Tecopa Lake		-1.5	20.5	gm carb sand - capping ls from outcrop top	00516827
HD-2211 b	TEC-120496-JW1	Tecopa Lake		-1.3	20.4	massive cal - tan micrite 1-2m from top	00516827
HD-2211 c	TEC-120496-JW1	Tecopa Lake		-1.8	20.7	creamy carb mud - dessicated cc mud rock	00516827
HD-2211 d	TEC-120496-JW1	Tecopa Lake		-1.9	20.2	oldest cal - silty chalky ls ~5m from top	00516827
HD-2212	TEC-120496-JW2	Tecopa Lake		-1.5	20.6	trav-like cal - sub-hriz lam'd trav vein from near	00516828

[1] - Depth below surface (in meters)

Table 1: Uranium-series disequilibrium results from past discharge deposits in the state line area.

Sample Name	Sample wt. (g)	Concentration U (ppm)	Concentration Th (ppm)	Measured Activity Ratios (2σ)[a] $^{234}U/^{238}U$	Measured Activity Ratios (2σ)[a] $^{230}Th/^{238}U$	Measured Activity Ratios (2σ)[a] $^{230}Th/^{232}Th$	Detritus-corrected $^{230}Th/U$ Age in ka (2σ)[b]	Detritus-corrected Initial $^{234}U/^{238}U$ Activity (2σ)[b]	Detritus-corrected $^{234}U/^{238}U$ Age in ka[c]	Sample Type
State Line Deposits - Mesquite Wash Section: Lat. 36°25'48"N; Long. 116°27'36"W.										
HD2198-B1	0.067	0.70	2.38	1.185 (0.010)	1.352 (0.024)	1.206 (0.023)	Excess 230Th	Excess 230Th		Paleo Spring Carbonate
HD2198-C1	0.083	0.61	2.38	1.221 (0.010)	1.341 (0.034)	1.045 (0.027)	Excessive 232Th	Excessive 232Th		Paleo Spring Carbonate
HD2199-C1	0.088	0.19	0.51	2.036 (0.022)	3.139 (0.061)	3.533 (0.073)	Excessive 232Th	Excessive 232Th		Paleo Spring Carbonate - Vein
HD2199-C2	0.087	0.22	0.74	2.330 (0.103)	5.038 (0.122)	4.448 (0.056)	Excessive Th	Excessive Th		Paleo Spring Carbonate
HD2200-A1	0.126	0.43	2.69	1.924 (0.022)	4.649 (0.040)	2.273 (0.027)	Excessive 232Th	Excessive 232Th		Nodular Carbonate
HD2200-D1	0.088	0.44	1.81	1.720 (0.010)	3.853 (0.042)	2.859 (0.039)	Excessive Th	Excessive Th		Nodular Carbonate
HD2201-A	0.052	11.42	1.48	2.645 (0.014)	2.153 (0.009)	50.51 (0.31)	142 (2)	3.55 (0.04)	66 {3.05}	Nodular Carbonate
HD2201-B	0.076	1.55	1.09	3.534 (0.019)	17.184 (0.075)	74.3 (3.1)	Excess 230Th	Undefined		Nodular Carbonate
HD2201-C	0.055	7.15	0.53	2.752 (0.014)	2.037 (0.016)	83.41 (0.74)	121 (2)	3.52 (0.03)	49 {3.05}	Rhizolith - Individual
HD2201-D	0.166	6.23	0.32	2.718 (0.014)	1.970 (0.008)	115.49 (0.61)	117.3 (1.3)	3.43 (0.02)	58 {3.05}	Rhizolith - Individual
HD2201-E	0.059	8.38	0.15	2.696 (0.013)	1.767 (0.021)	303.5 (4.3)	100.8 (1.9)	3.267 (0.017)	65 {3.05}	Rhizolith - Individual
HD2202-A	0.117	2.30	0.70	3.088 (0.017)	5.042 (0.026)	50.12 (0.63)	Excess 230Th	Undefined	Undefined	Nodular Carbonate
HD2202-B	0.060	1.74	0.98	3.625 (0.028)	16.40 (0.12)	88.40 (0.83)	Excess 230Th	Undefined	Undefined	Nodular Carbonate
HD2202-C	0.071	9.01	1.38	2.670 (0.014)	2.480 (0.016)	49.27 (0.47)	183 (4)	3.9 (0.1)	58 {3.05}	Nodular Carbonate
State Line Deposits - High Terrace above Mesquite Wash: Lat. 36°26'04.9"N; Long. 116°27'19.4"W.										
HD2203-A	0.067	0.62	0.34	1.709 (0.011)	1.614 (0.019)	9.02 (0.13)	204 (15)	2.47 (0.12)	321 {3.05}	Paleo Spring Carbonate
HD2203-B	0.051	0.51	0.99	1.914 (0.020)	2.127 (0.025)	3.323 (0.045)	324 (110)	5.6 (2.6)		Paleo Spring Carbonate
HD2204-A	0.042	0.42	1.16	2.022 (0.018)	3.455 (0.072)	3.788 (0.079)	Excess Th	Undefined		Paleo Spring Carbonate/Opal
HD2204-B	0.054	0.43	0.12	1.722 (0.031)	1.963 (0.024)	20.5 (2.0)	438 (93)	3.7 (0.6)	341 {3.05}	Paleo Spring Carbonate/Opal
HD2205-A	0.078	0.40	0.44	1.39 (0.03)	1.165 (0.023)	3.282 (0.064)	149 (+42/-31)	1.8 (0.2)	466 {3.05}	Paleo Spring Carbonate
HD2205-B	0.085	0.60	1.16	1.340 (0.011)	1.569 (0.093)	2.46 (0.15)	Excess 230Th	Undefined	389 {3.05}	Paleo Spring Carbonate
State Line Deposits - Hectorite clay pit south of Franklin Well: Lat. 36°25'22"N; Long. 116°28'00"W.										
HD2206-A	0.100	0.14	0.15	1.863 (0.028)	1.884 (0.058)	5.20 (0.16)	235 (41)	3.3 (0.5)	188 {3.05}	Hectorite ore - bulk rock

Table 1: Uranium-series disequilibrium results from past discharge deposits in the state line area.

Sample Name	Sample wt. (g)	Concentration U (ppm)	Concentration Th (ppm)	Measured Activity Ratios (2σ)[a] $^{234}U/^{238}U$	$^{230}Th/^{238}U$	$^{230}Th/^{232}Th$	Detritus-corrected $^{230}Th/U$ Age in ka (2σ)[b]	Initial $^{234}U/^{238}U$ Activity (2σ)[b]	$^{234}U/^{238}U$ Age in ka[c]	Sample Type
State Line Deposits - Scranton Well Section: Lat. 36°27'06"N; Long. 116°30'10"W.										
HD2208a-1	0.108	1.35	1.41	2.567 (0.018)	1.193 (0.016)	3.457 (0.069)	53 (8)	3.5 (0.4)		Paleo Spring Carbonate
HD2208a-2	0.072	1.75	1.62	2.543 (0.014)	0.927 (0.006)	3.044 (0.027)	37 (7)	3.3 (0.3)		Paleo Spring Carbonate - bulk rock
HD2208b-1	0.060	4.54	0.14	2.837 (0.019)	1.258 (0.013)	127.2 (3.2)	59.2 (0.9)	3.19 (0.02)		Paleo Spring Carbonate - vein
HD2208b-2	0.061	0.69	1.32	2.524 (0.015)	1.884 (0.021)	2.999 (0.042)	106 (18)	5.0 (1.9)	54 {4.50}	Paleo Spring Carbonate - bulk rock
HD2208c1-A	0.144	1.11	2.18	2.413 (0.015)	1.593 (0.017)	2.464 (0.034)	82 (18)	4.6 (1.7)		Paleo Spring Carbonate
HD2208c1-B	0.096	1.14	2.15	2.303 (0.016)	1.567 (0.094)	2.51 (0.15)	87 (21)	4.3 (1.5)		Paleo Spring Carbonate - bulk rock
HD2208c2-A	0.115	1.18	1.53	2.650 (0.014)	1.737 (0.013)	4.06 (0.06)	89 (10)	4.2 (0.8)		Paleo Spring Carbonate - bulk rock
	0.125	1.03	2.40	2.492 (0.014)	1.911 (0.016)	2.48 (0.03)	106 (23)	6.1 (3.7)		Paleo Spring Carbonate

[a] Measured isotope ratios corrected for mass fractionation, spike contributions, procedural blank and normalized relative to a standard value for NIST SRM 4321b $^{234}U/^{238}U=0.0000529$.

[b] $^{230}Th/U$ age, initial $^{234}U/^{238}U$ ratio and associated errors calculated after correcting for Th correction using ISOPLOT, version 2.91 (Ludwig, K.R., 1991, U.S. Geol. Surv. OFR 91-445, 42 p.).

Assumed Th-bearing detrital component has an atomic Th/U of 4 with the following activity ratios and 2σ errors: $^{232}Th/^{238}U=1.276\pm0.64$; $^{234}U/^{238}U=1.0\pm0.1$; and $^{230}Th/^{238}U=1.0\pm0.25$.

[c] Model $^{234}U/^{238}U$ age calculated from the detritus-corrected $^{234}U/^{238}U$ acitivity ratio assuming the initial isotopic compositions listed in brackets.

Table 2: Thermoluminescence results from paleo discharge deposits. All errors given at the 95% confidence limit.

Sample Name	Moisture Content		Dose Rate (Gy/ka)		Total Bleach	Total Bleach Age (ka)				Partial Bleach	Partial Bleach Age (ka)			
	Field (%)	Saturated (%)	Field Moist.	Saturated Moist.	Equivalent Dose (Gy)	Field Moist DR	½ Satura. Moist DR	Saturated Moist DR	Total Range	Eqivalent Dose (Gy)	Field Moist DR	½ Satura. Moist DR	Saturated Moist DR	Total Range
TL-44	*[SLD Mesquite Wash section: greenish gray fine-sand with small white nodules and sub horiz., white stringers near top. Sample from 360 cm below terrace surface]*													
	2.8	61	9.8 ± 0.6	5.7 ± 0.4	689 ± 121	70 ± 13	94 ± 18	120 ± 23	57-143	901 ± 180	92 ± 19	123 ± 26	158 ± 33	73-191
TL-45	*[SLD Mesquite Wash section: moderately hard, cream-colored fine-sand with evenly spaced vertical tubular cavities. Sample from 220 cm below terrace surface]*													
	3.4	58	11.3 ± 0.8	6.7 ± 0.5	224 ± 14	20 ± 1.8	26 ± 3	33 ± 3	18-36	250 ± 13	22 ± 1.9	30 ± 3	37 ± 4	20-41
TL-46	*[SLD Amargosa River snail site: brown, silty deposits associated with 9-11ka snails. Sample from ~0.4 m below surface.]*													
	22	45	5.4 ± 0.5	4.4 ± 0.5	65 ± 4	12 ± 1.4	nd	15 ± 1.8	11-17	59 ± 7.8	11 ± 1.8	nd	13 ± 2.3	9-15
TL-84	*[SLD Mesquite Wash section: greenish brown fine-sand with granular appearance. Sample from 480 cm below terrace surface]*													
	1.7	77	6.5 ± 0.4	3.5 ± 0.3	635 ± 23	98 ± 8	142 ± 11	184 ± 15	90-199	na	na	na	na	na
TL-85	*[SLD Mesquite Wash section: unconsolidated, brownish fine-sand. Sample from 525 cm below terrace surface]*													
	2.3	57	6.5 ± 0.4	3.5 ± 0.3	965 ± 82	149 ± 16	216 ± 24	279 ± 32	133-311	na	na	na	na	na
TL-86	*[SLD Amargosa River snail site: brown, silty deposits associated with 9-11ka snails. Samplel from auger hole at a depth of 3.2 m below surface.]*													
	17	70	5.5 ± 0.4	3.6 ± 0.3	61 ± 4	11 ± 1.0	14 ± 1.3	17 ± 1.6	10-19	46 ± 10	8.4 ± 1.9	10 ± 2	13 ± 3	7-16
TL-87	*[CFW, central area: greenish sand just below a low bench of hard, punky green sandy root-rich material. Sample from a depth of about 25 cm below local surface.]*													
	7.4	53	7.4 ± 0.5	4.9 ± 0.4	110 ± 14	15 ± 2	18 ± 3	22 ± 3	13-25	na	na	na	na	na

na = not available
nd = not determined
DR = Dose Rate

Table 3: Sr isotopic compositions of HCl leachates.

Sample	[Sr] ppm	$^{87}Sr/^{86}Sr$	$\delta^{87}Sr^{*}$ (‰)
Lathrop Wells Diatomite Station 6 Section: Lat. 35°42'28"N; Long. 116°35'15"W.			
HD1972-U4 HCl-L(S)	217.0	0.71275	5.01
State Line Deposits - Mesquite Wash Section: Lat. 36°25'48"N; Long. 116°27'36"W.			
HD2202-C HCl-L(S)	1940	0.71667	10.53
HD2201-A HCl-L(S)	1484	0.71685	10.79
HD2200-D1 HCl-L(S)	101.6	0.71758	11.82
HD2200-A HCl-L(S)	111.2	0.71743	11.60
HD2199-C2 HCl-L(S)	93.65	0.71765	11.91
HD2199-C1 HCl-L(S)	51.36	0.71786	12.21
HD2198-C1 HCl-L(S)	270.1	0.71712	11.17
HD2198-B HCl-L(S)	286.7	0.71683	10.76
State Line Deposits - High Terrace above Mesquite Wash: Lat. 36°26'04.9"N; Long. 116°27'19.4"W.			
HD2203-A HCl-L(S)	245.3	0.71706	11.08
HD2203-B HCl-L(S)	697.4	0.7166	10.43
HD2204-B HCl-L(S)	454.9	0.7182	12.69

$$^{*}\delta^{87}Sr = \left[\left(\frac{^{87}Sr/^{86}Sr_{meas.}}{^{87}Sr/^{86}Sr_{s.w}}\right) - 1\right] * 1000$$

where

$^{87}Sr/^{86}Sr_{s.w} = 0.70920$

Table 4: Uranium-series disequilibrium results from Lathrop Wells Diatomite.

Sample Name	Sample wt. (g)	Concentration U (ppm)	Concentration Th (ppm)	Measured Activity Ratios (2σ)[a] $^{234}U/^{238}U$	Measured Activity Ratios (2σ)[a] $^{230}Th/^{238}U$	Measured Activity Ratios (2σ)[a] $^{230}Th/^{232}Th$	Detritus-corrected $^{230}Th/U$ Age in ka (2σ)[b]	Detritus-corrected Initial $^{234}U/^{238}U$ Activity (2σ)[b]	$^{234}U/^{238}U$ Age in ka[c]	Sample Type
Lathrop Wells Diatomite Station 6 Section: Lat. 35°42'28"N; Long. 116°35'15"W.										
HD1970-U3	0.021	4.01	4.72	3.175 (0.028)	1.414 (0.013)	3.648 (0.074)	50 (7)	4.6 (0.7)	-14 {4.00}	Small plant petrifaction
HD1970-U4	0.014	11.00	5.64	3.393 (0.025)	2.298 (0.036)	13.59 (0.24)	101 (4)	4.7 (0.3)	30 {4.00}	Small plant petrifaction
HD1970-U5	0.003	13.51	4.46	3.399 (0.025)	0.982 (0.011)	9.02 (0.11)	33 (2)	3.88 (0.13)	47 {4.00}	Small plant petrifaction
HD1970-U6	0.017	4.82	4.57	3.225 (0.028)	1.511 (0.080)	4.84 (0.26)	56 (7)	4.5 (0.5)	6 {4.00}	Composite plant petrifactions
HD1971-U3	0.028	0.42	0.69	2.436 (0.024)	2.222 (0.024)	4.147 (0.053)	165 (22)	5.0 (1.4)	25 {3.66}	Small plant petrifaction
HD1971-U4	0.049	5.55	1.78	3.117 (0.018)	1.254 (0.083)	11.87 (0.83)	50 (5)	3.66 (0.12)	50 {3.66}	Small plant petrifaction
HD1971-U5	0.041	1.79	3.19	2.265 (0.016)	1.89 (0.21)	3.23 (0.36)	135 (40)	4.4 (1.4)	45 {3.66}	Small white nodule
HD1972-U1r	0.019	6.01	5.79	2.625 (0.036)	2.459 (0.026)	7.73 (0.19)	180 (14)	4.6 (0.6)		Nodular Carbonate
HD1972-U2r	0.070	9.46	1.16	2.547 (0.015)	2.569 (0.025)	63.34 (0.77)	223 (7)	4.00 (0.07)	178 {3.65}	Nodular Carbonate
HD1972-U3	0.043	3.77	0.57	2.676 (0.017)	2.776 (0.024)	55.27 (0.53)	237 (7)	4.41 (0.09)	179 {3.90}	Nodular Carbonate
HD1972-U4	0.064	4.58	0.72	2.478 (0.026)	2.714 (0.024)	52.71 (0.57)	283 (14)	4.44 (0.12)	185 {3.60}	Nodular Carbonate

[a] Measured isotope ratios corrected for mass fractionation, spike contributions, procedural blank and normalized relative to a standard value for NIST SRM 4321b $^{234}U/^{238}U=0.0000529$.

[b] $^{230}Th/U$ age, initial $^{234}U/^{238}U$ ratio and associated errors calculated after correcting for Th correction using ISOPLOT, version 2.91 (Ludwig, K.R., 1991, U.S. Geol. Surv. OFR 91-445, 42 p.).

Assumed Th-bearing detrital component has an atomic Th/U of 4 with the following activity ratios and 2σ errors: $^{232}Th/^{238}U=1.276\pm0.64$; $^{234}U/^{238}U=1.0\pm0.1$; and $^{230}Th/^{238}U=1.0\pm0.25$.

[c] Model $^{234}U/^{238}U$ age calculated from the detritus-corrected $^{234}U/^{238}U$ acitivity ratio assuming the initial isotopic compositions listed in brackets.

TABLE 6: U-Th isotope analyses with calculated ages and initial uranium isotopic compositions.

Sample Name	Sample wt. (g)	Concentration U (ppm)	Concentration Th (ppm)	Measured Activity Ratios[a] $^{234}U/^{238}U$ (2σ)	Measured Activity Ratios[a] $^{230}Th/^{238}U$ (2σ)	Measured Activity Ratios[a] $^{230}Th/^{232}Th$ (2σ)	Detritus-corrected values $^{230}Th/U$ Age in ka (2σ)[b]	Detritus-corrected values Initial $^{234}U/^{238}U$ Activity (2σ)[b]	Detritus-corrected values $^{234}U/^{238}U$ Age in ka[c]	Sample Type
Unit 3f modern soil, Fortymile Canyon: Latitude 36°56'08"N; Longitude 116°22'35"W										
HD2122-A1	0.0369	7.54	6.94	1.855 (0.010)	0.620 (0.006)	2.05 (0.02)	29 (9)	2.22 (0.17)		Si-rich Clast Rind
HD2122-A2	0.0599	20.8	0.81	1.852 (0.010)	0.3462 (0.0019)	27.1 (0.2)	21.6 (0.4)	1.914 (0.011)		Individual Rhizolith
HD2122-B1	0.0437	20.0	2.42	1.847 (0.010)	0.459 (0.003)	11.46 (0.10)	28.6 (1.1)	1.95 (0.02)		Si-rich Clast Rind
Unit 3f modern soil, Calico Fan: Latitude 36°48'51.5"N; Longitude 116°23'52"W										
HD1743-A1	0.0682	7.24	0.67	1.497 (0.008)	0.476 (0.004)	15.69 (0.14)	39.1 (1.1)	1.568 (0.012)		Si-rich stringer in rootlet Mass
HD1743-A2	0.1173	4.61	1.65	1.464 (0.006)	0.628 (0.006)	5.31 (0.06)	52 (5)	1.59 (0.03)		Si-rich stringer in rootlet Mass
HD1743-A3	0.1435	19.1	0.09	1.474 (0.009)	0.258 (0.002)	163.6 (1.2)	20.6 (0.2)	1.503 (0.010)		Si-rich stringer in rootlet Mass
HD1743-A4	0.0468	11.6	0.08	1.487 (0.008)	0.487 (0.003)	225 (4)	42.1 (0.5)	1.550 (0.009)		Si-rich stringer in rootlet Mass
Unit 3f buried soil, Calico Fan: Latitude 36°48'51.5"N; Longitude 116°23'52"W										
HD1742-B1	0.1311	18.7	0.08	1.400 (0.007)	0.530 (0.003)	359 (3)	50.4 (0.5)	1.4610 (0.01)		Individual Rhizolith
HD1742-B2	0.1494	8.06	0.20	1.488 (0.008)	0.799 (0.005)	95.3 (0.8)	79.1 (1.0)	1.6140 (0.01)		Individual Rhizolith
HD1742-B3	0.239	6.94	0.45	1.502 (0.011)	0.676 (0.005)	31.7 (0.3)	61.5 (1.2)	1.6080 (0.01)		Individual Rhizolith
Unit 3f buried soil, Fortymile Wash high terrace at Powerline Eolianite: Latitude 36°50'11"N; Longitude 116°23'21"W										
HD1739-A1	0.0596	9.35	1.34	1.210 (0.007)	1.101 (0.007)	23.4 (0.2)	220 (9)	1.41 (0.02)	357 {1.6}	Carbonate-rich fine-rootlet Mass
HD1739-A3	0.0345	28.1	0.14	1.274 (0.007)	1.252 (0.006)	780 (11)	279 (9)	1.60 (0.02)	277 {1.6}	Si-rich lens in fine-rootlet mass
Unit 3f modern soil, Fortymile Wash high terrace at Sever Wash Gooseneck: Latitude 36°49'36"N; Longitude 116°24'01.5"W										
HD1916-A2	0.0008	4.46	0.43	1.82 (0.13)	0.43 (0.03)	14 (2)	27 (3)	1.91 (0.13)		Late, clear opal on innermost rind
HD1916-B	0.0291	3.05	2.35	1.700 (0.010)	0.573 (0.003)	2.26 (0.02)	30 (8)	1.95 (0.10)		Innermost Si-rich Rind
HD1916-C	0.0287	12.0	2.51	1.721 (0.011)	0.910 (0.005)	13.21 (0.10)	74 (3)	1.94 (0.03)		Innermost Si-rich Rind
Unit 3f buried soil, Fortymile Wash high terrace at Sever Wash Gooseneck: Latitude 36°49'36"N; Longitude 116°24'01.5"W										
HD1740-A	0.0326	5.11	2.23	1.410 (0.010)	0.870 (0.007)	6.03 (0.06)	90 (7)	1.60 (0.04)		Individual Rhizolith
HD1740-B	0.0116	10.4	4.57	1.394 (0.011)	0.956 (0.011)	6.63 (0.08)	108 (8)	1.60 (0.04)		Individual Rhizolith
HD1740-C	0.0786	6.79	1.63	1.421 (0.008)	0.871 (0.010)	11.0 (0.2)	93 (4)	1.58 (0.02)		Individual Rhizolith
HD1740-D	0.0343	3.82	4.11	1.360 (0.009)	0.960 (0.008)	2.71 (0.02)	101 (21)	1.66 (0.12)		Individual Rhizolith
Unit 3f 1st buried soil, Fortymile Wash high terrace at Sever Wash Gooseneck: Latitude 36°49'36"N; Longitude 116°24'01.5"W										
HD1741-B	0.0154	18.0	3.04	1.469 (0.009)	1.244 (0.007)	22.40 (0.18)	169 (5)	1.79 (0.02)		Innermost Si-rich Rind
HD1741-C	0.0564	32.5	1.89	1.398 (0.008)	1.174 (0.006)	61.3 (0.4)	170 (3)	1.654 (0.010)		Innermost Si-rich Rind
HD1741-E	0.0504	17.3	3.52	1.351 (0.008)	1.079 (0.022)	16.1 (0.3)	152 (8)	1.57 (0.02)		Innermost Si-rich Rind
Unit 3f modern soil, Fortymile Wash high terrace at N85: Latitude 36°48'42"N; Longitude 116°23'50"W										
HD1375-A1	0.0919	9.06	4.67	1.489 (0.007)	0.651 (0.008)	3.83 (0.05)	51 (7)	1.65 (0.06)	76 {1.7}	Si-rich stringer in detrital matrix
HD2136-B1	0.037	9.81	1.92	1.571 (0.008)	0.650 (0.003)	10.08 (0.06)	53 (2)	1.70 (0.02)	54 {1.7}	Si-rich Clast Rind
HD2136-D1	0.0504	12.1	2.74	1.58 (0.03)	0.629 (0.005)	8.40 (0.08)	49 (3)	1.71 (0.04)	42 {1.7}	Si-rich Clast Rind
HD2136-E1	0.0512	9.92	1.29	1.585 (0.008)	0.574 (0.005)	13.40 (0.15)	45.3 (1.5)	1.688 (0.014)	52 {1.7}	Si-rich Clast Rind

Sample Name	Sample wt. (g)	Concentration U (ppm)	Concentration Th (ppm)	Measured Activity Ratios[a] $^{234}U/^{238}U$ (2σ)	Measured Activity Ratios[a] $^{230}Th/^{238}U$ (2σ)	Measured Activity Ratios[a] $^{230}Th/^{232}Th$ (2σ)	Detritus-corrected values $^{230}Th/U$ Age in ka (2σ)[b]	Detritus-corrected values Initial $^{234}U/^{238}U$ Activity (2σ)[b]	$^{234}U/^{238}U$ Age in ka[c]	Sample Type
HD2136-F1	0.049	9.93	2.37	1.548 (0.008)	0.708 (0.005)	9.02 (0.07)	60 (3)	1.69 (0.02)	64 {1.7}	Si-rich Clast Rind
Unit 3f 1st buried soil, Fortymile Wash high terrace at N85: Latitude 36°48'42"N; Longitude 116°23'50"W										
HD2135-A1	0.0607	9.39	0.85	1.385 (0.007)	1.508 (0.010)	50.3 (0.4)	449 (+61/-45)	2.4 (0.2)	203 {1.7}	Si-rich Clast Rind
HD2135-B1	0.0495	8.92	2.30	1.445 (0.008)	1.494 (0.009)	17.57 (0.17)	305 (21)	2.13 (0.07)	136 {1.7}	Si-rich Clast Rind
HD2135-C1	0.0519	14.0	0.62	1.464 (0.008)	1.555 (0.008)	106.5 (0.9)	347 (16)	2.25 (0.04)	141 {1.7}	Si-rich Clast Rind
HD2135-D1	0.0761	5.72	0.52	1.392 (0.008)	1.545 (0.008)	51.3 (0.3)	567 (+200/-94)	3.0 (0.8)	197 {1.7}	Si-rich Clast Rind
Unit 3f 2nd buried soil, Fortymile Wash high terrace at N85: Latitude 36°48'42"N; Longitude 116°23'50"W										
HD2134-B1	0.0523	26.2	1.72	1.124 (0.006)	1.224 (0.006)	56.7 (0.4)	Excess 230Th	Undefined	606 {1.7}	Si-rich Clast Rind
HD2134-C1	0.0622	13.3	2.00	1.160 (0.006)	1.228 (0.007)	24.80 (0.19)	729 (***)	2.3 (***)	507 {1.7}	Si-rich Clast Rind
HD2134-D1	0.0396	8.47	1.47	1.182 (0.006)	1.222 (0.009)	21.35 (0.17)	411 (+74/-51)	1.61 (0.10)	459 {1.7}	Si-rich Clast Rind
Unit 3f buried eolian sand, Fortymile Wash high terrace at N85: Latitude 36°48'42"N; Longitude 116°23'50"W										
HD2133-B1	0.0671	9.19	0.31	1.225 (0.007)	1.405 (0.010)	127.9 (1.0)	Excess 230Th	Undefined	398 {1.7}	Individual Rhizolith
HD2133-C1	0.0944	10.1	0.29	1.205 (0.007)	1.382 (0.019)	147 (2)	Excess 320Th	Undefined	431 {1.7}	Individual Rhizolith
Unit 4f modern soil, Fortymile Wash inset terrace: Latitude 36°49'12"N; Longitude 116°23'48"W										
HD2124-B1	0.057	17.7	3.23	1.912 (0.010)	0.467 (0.002)	7.75 (0.05)	27.2 (1.6)	2.03 (0.03)		Si-rich Clast Rind
HD2124-D1	0.0526	16.6	3.32	1.876 (0.010)	0.498 (0.003)	7.55 (0.05)	29.8 (1.8)	2.01 (0.03)		Si-rich Clast Rind
HD2124-E1	0.0549	12.8	4.79	1.879 (0.010)	0.545 (0.004)	4.42 (0.04)	31 (3)	2.06 (0.05)		Si-rich Clast Rind
Unit 4f modern soil, Fortymile Wash inset terrace: Latitude 36°48'51.5"N; Longitude 116°23'52"W										
HD2123-D1	0.0495	8.03	1.62	1.931 (0.010)	0.419 (0.003)	6.29 (0.06)	23.2 (1.7)	2.05 (0.03)		Si-rich Clast Rind
HD2123-F1	0.065	29.4	2.86	2.391 (0.016)	0.706 (0.004)	22.0 (0.2)	35.7 (0.8)	2.58 (0.03)		Si-rich Clast Rind
HD2123-G1	0.0564	10.6	6.65	1.851 (0.011)	0.511 (0.003)	2.48 (0.02)	25 (6)	2.09 (0.09)		Si-rich Clast Rind
HD2123-H1	0.0648	9.55	3.08	1.809 (0.010)	0.394 (0.002)	3.71 (0.03)	21 (3)	1.94 (0.04)		Si-rich Clast Rind
Unit 3f modern soil, Fortymile Wash high terrace at Gate 510 quarry: Latitude 36°39'50"N; Longitude 116°24'28"W										
HD2137-B1	0.0654	9.13	0.67	1.652 (0.009)	0.892 (0.006)	36.7 (0.4)	78.3 (1.3)	1.829 (0.013)		Si-rich Clast Rind
HD2137-C1	0.0627	13.8	1.19	1.647 (0.010)	0.862 (0.005)	30.2 (0.3)	74.8 (1.3)	1.817 (0.014)		Si-rich Clast Rind
HD2137-D1	0.0452	10.7	0.94	1.616 (0.065)	0.891 (0.012)	30.7 (0.3)	81 (5)	1.79 (0.07)		Si-rich Clast Rind
Unit 3f modern soil, Fortymile Wash high terrace at Hwy 95 quarry: Latitude 36°39'25"N; Longitude 116°26'51"W										
HD2138-B1	0.0542	24.2	1.99	1.838 (0.011)	0.1689 (0.0012)	6.21 (0.07)	9.2 (0.7)	1.879 (0.014)		Si-rich Clast Rind
HD2138-C1	0.0479	18.8	1.94	1.796 (0.011)	0.1605 (0.0010)	4.71 (0.05)	8.5 (0.9)	1.838 (0.015)		Si-rich Clast Rind
HD2138-D1	0.0459	12.1	7.82	1.876 (0.011)	0.268 (0.003)	1.26 (0.02)	7 (6)	2.07 (0.10)		Si-rich Clast Rind

[a] Measured isotope ratios corrected for mass fractionation, spike contributions, procedural blank and normalized relative to a standard value for NIST SRM 4321b $^{234}U/^{238}U=0.0000529$.

[b] $^{230}Th/U$ age, initial $^{234}U/^{238}U$ ratio and associated errors calculated after correcting for Th correction using ISOPLOT, version 2.91 (Ludwig, K.R., 1991, U.S. Geol. Surv. OFR 91-445, 42 p.). Assumed Th-bearing detrital component has an atomic Th/U of 4 with the following activity ratios and 2σ errors: $^{232}Th/^{238}U=1.276\pm0.64$; $^{234}U/^{238}U=1.0\pm0.1$; and $^{230}Th/^{238}U=1.0\pm0.25$.

[c] Model $^{234}U/^{238}U$ age calculated from the measured $^{234}U/^{238}U$ acitivity ratio assuming the initial isotopic compositions listed in brackets.

Table 7: Thermoluminescence results from alluvial deposits of Fortymile Wash at Highway 95. All errors given at the 95% confidence limit.

Sample Name	Moisture Content		Dose Rate (Gy/ka)		Total Bleach	Total Bleach Age (ka)				Partial Bleach	Partial Bleach Age (ka)			
	Field (%)	Saturated (%)	Field Moist.	Saturated Moist.	Equivalent Dose (Gy)	Field Moist DR	½ Satura. Moist DR	Saturated Moist DR	Total Range	Eqivalent Dose (Gy)	Field Moist DR	½ Satura. Moist DR	Saturated Moist DR	Total Range
TL-79	*[Gravel Pit along Hwy 95, ~4.5 km west of Amargosa Valley: brown, bedded fine sand with calcite-cemented layers. From ~50 cm depth below local surface.]*													
	2.2	40	7.9 ± 0.5	5.4 ± 0.4	55 ± 3	7.0 ± 0.6	8.8 ± 0.7	10.1 ± 0.9	6-11	42 ± 7	5.3 ± 0.9	6.7 ± 1.2	7.8 ± 1.4	4-9
TL-80	*[Gravel Pit along Hwy 95, ~4.5 km west of Amargosa Valley: greyish-brown, non-bedded fine sand. From ~15-20 cm depth below local surface.]*													
	1.3	25	8.4 ± 0.5	6.5 ± 0.4	49 ± 3	5.8 ± 0.5	nd	7.6 ± 0.7	5-8	23 ± 3	2.7 ± 0.4	nd	3.5 ± 0.5	2-4
TL-81	*[Gravel Pit along Hwy 95, ~4.5 km west of Amargosa Valley: greyish-brown, non-bedded fine sand. From ~15-20 cm depth below local surface.]*													
	2.6	32	8.6 ± 0.6	6.3 ± 0.4	316 ± 14	37 ± 3	nd	50 ± 4.1	34-54	269 ± 27	32 ± 4	nd	43 ± 5	28-48

nd = not determined
DR = Dose Rate

Table 8: Characteristic isotopic compositions of paleodischarge deposits, waters and rocks representing possible source materials.

Material	Initial $^{234}U/^{238}U_{activity}$	$\delta^{87}Sr$ (‰)	$\delta^{13}C$ (‰)
Paleodischarge deposits			
inorganic carbonate	2.9 to 4.5	5.0 to 13	-4 to +1
plant/mollusc	*	*	-10 to -5
Aquifers			
Paleozoic	2.5 to 4	3 to >10	-4 to -2 (HCO_3^-)*
Volcanic/alluvium	3 to 8	1 to 4 (no Precambrian) 7 to >15 (w/ Precambrian)	-13 to -7 (HCO_3^-)*
Perched waters at YM	3 to 7	3.5 to 4.5	-11 to -9 (HCO_3^-)*
Surface Waters at YM	1.4 to 1.8	1.8 to 3.8	
Rocks			
Marine carbonate	~1.0	-2 to +3**	-2 to +2
Calcrete	1.3 to 1.8	3.3 to 5.0	-10 to -5
Volcanics	~1.0	-1.3 to 15	negligible contribution
Precambrian siliciclastics	~1.0	10 to >30	negligible contribution

* At near-surface temperatures, the equilibrium d13C difference between dissolved HCO3- and calcite is ~2‰

** In areas of Paleozoic limestone that have been hydrothermally-altered, such as Bare Mountain, $\delta^{87}Sr$ values have been elevated to values from +23 to +30 through addition of radiogenic Sr derived from the Precambrian basement (Peterman et al., 1994).

Table 9: Matrix of possible hydrogenic sources and their compatibility with observed data from paleodischarge sites.

Hydrogenic Source	Initial $^{234}U/^{238}U_{activity}$	$\delta^{87}Sr$ (‰)	$\delta^{13}C$ (‰)	Diatoms
Paleozoic Aquifer	possible	possible	possible	unlikely
Volcanic/Alluvial Aquifer	possible	possible	possible	probable
Perched Aquifer	unlikely	NO	NO	NO
Surface Runoff	NO	NO	NO	NO

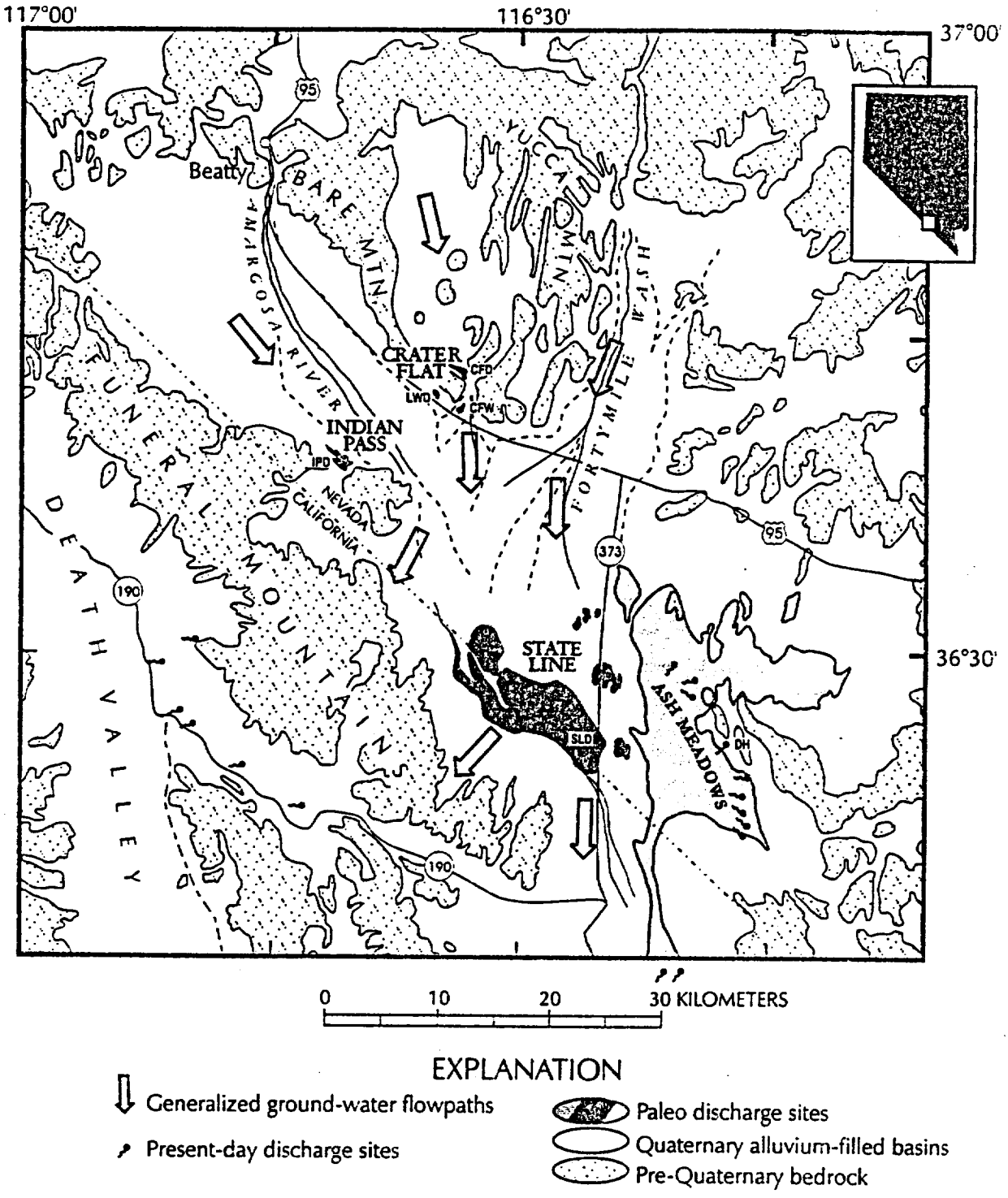

Figure 1: Location map showing Amargosa discharge deposits.

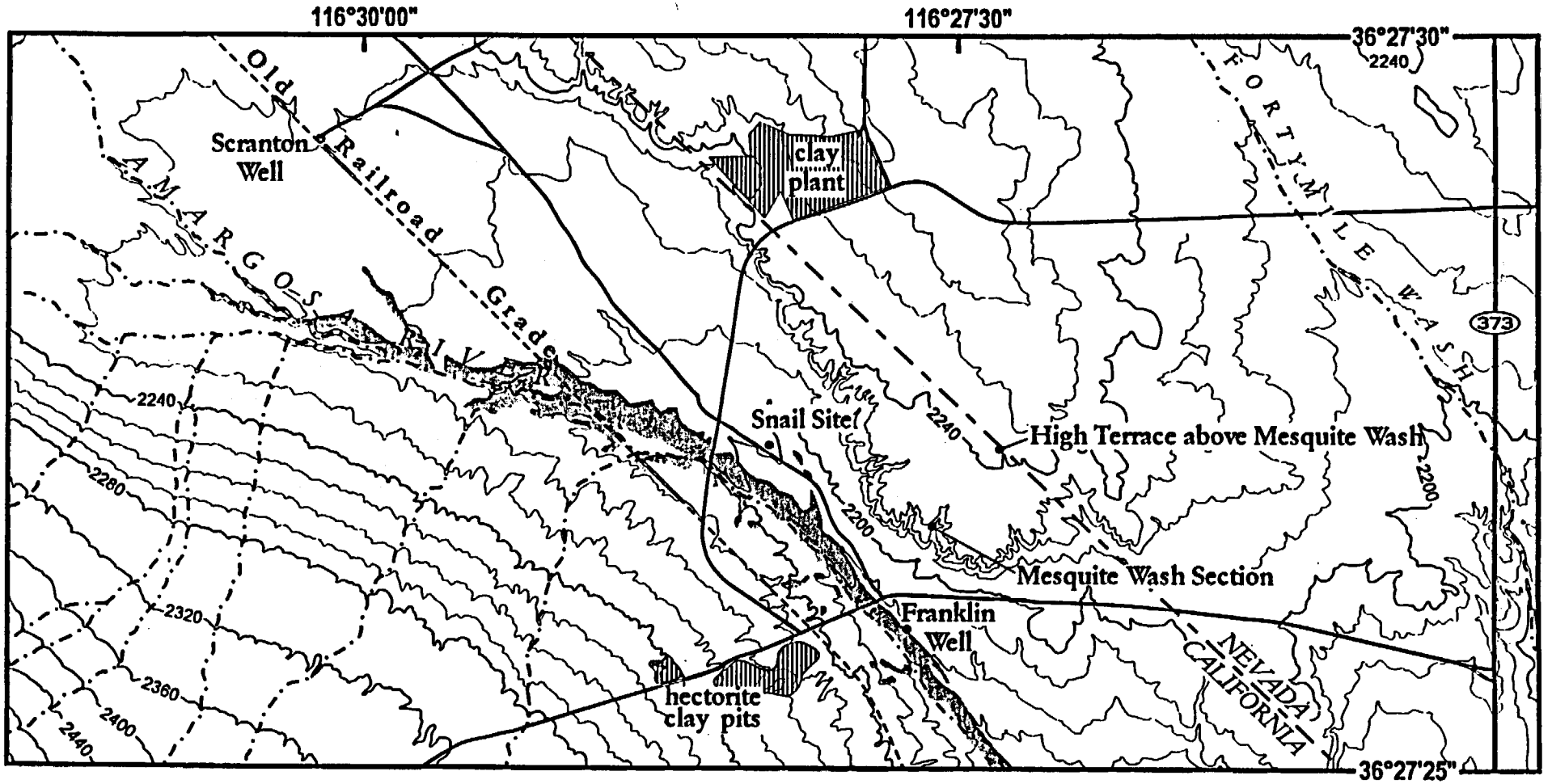

FIGURE 2: Topographic map of the Franklin Well and Scranton Well area. Shaded areas represent mesquite thickets along the Amargosa River Bottom.

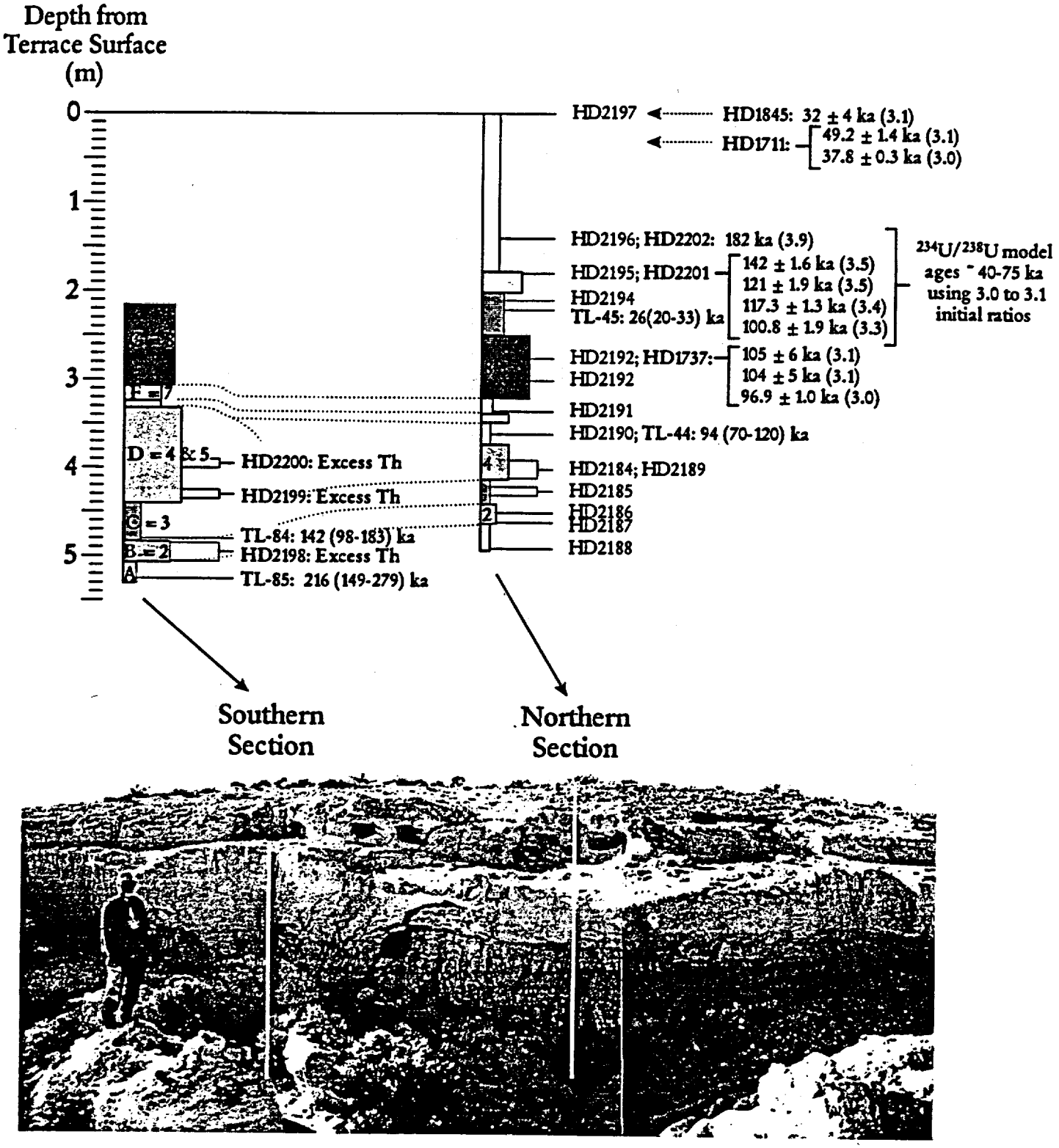

Figure 3: Generalized sections showing sample locations and corresponding ages for state line deposits at Mesquite Wash.

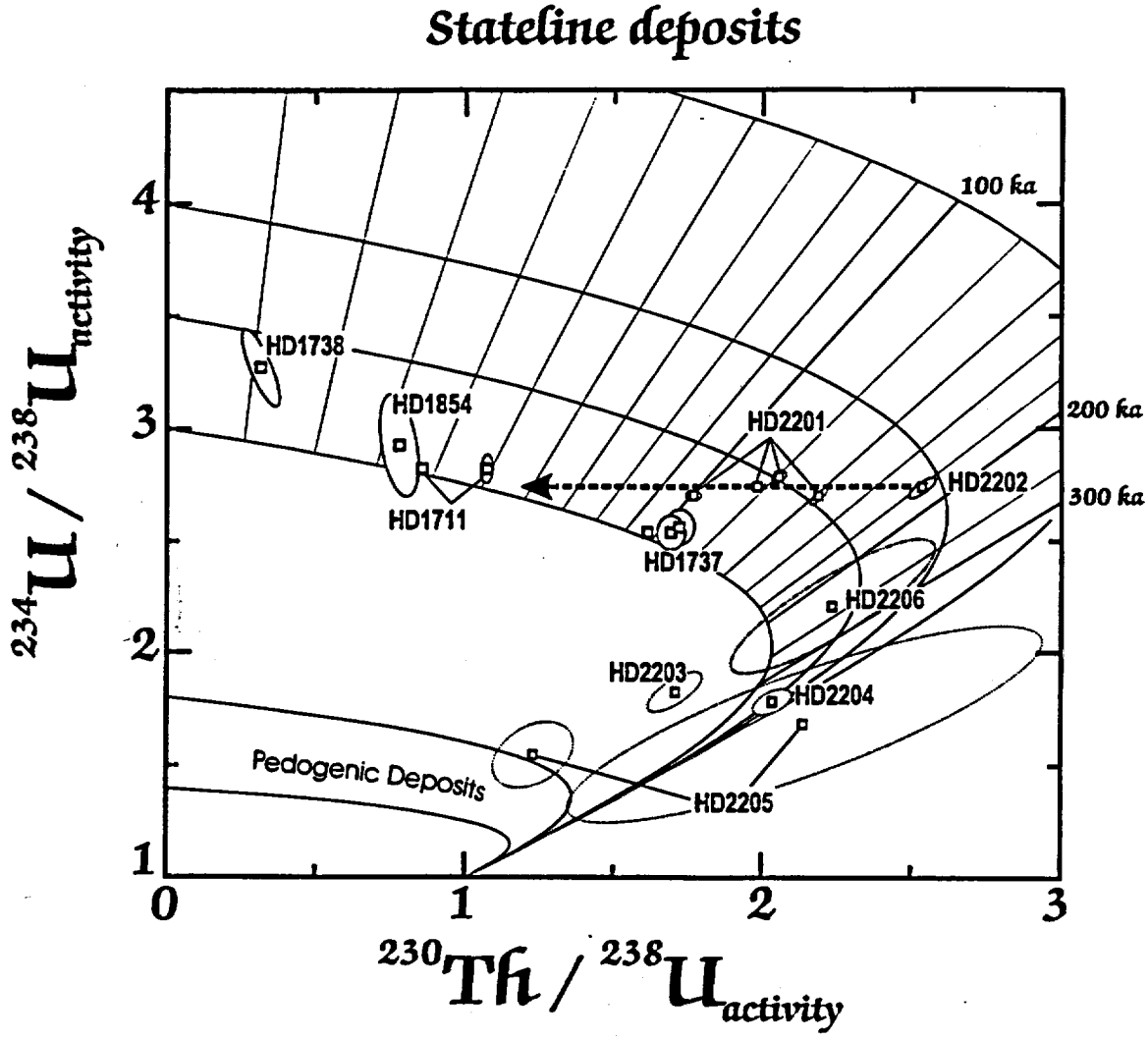

Figure 4: U-series evolution diagram showing U and Th isotopic results for data from State Line Deposits near Franklin Well.

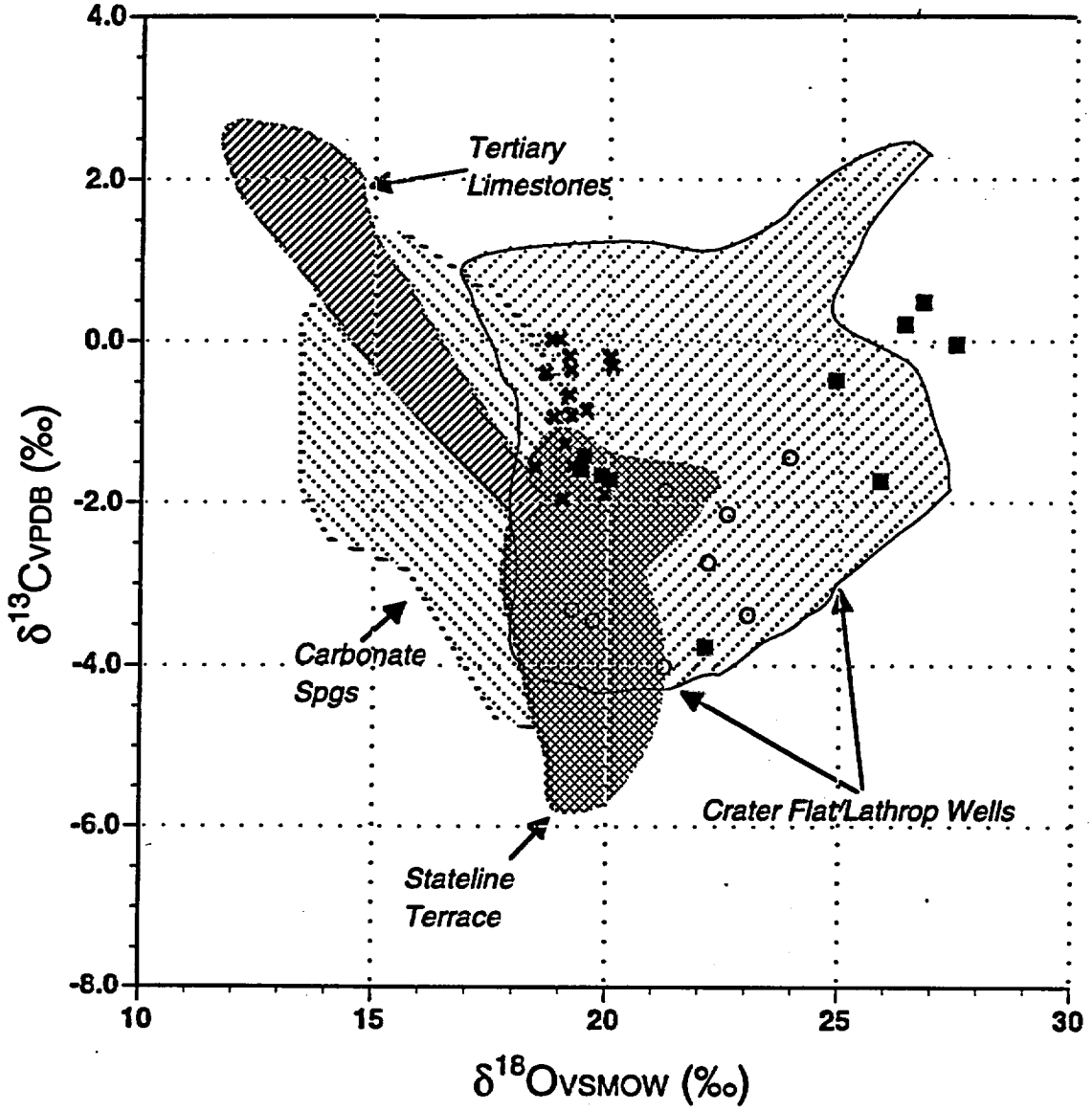

Fig 5. Plot of new $\delta^{13}C$ and $\delta^{18}O$ data of carbonates from stratigraphic sequences collected at the Stateline greenbed (O) and terrace (■) deposits, and Scranton Well (✱). Shown for reference are fields defined by preexisting data from spring carbonate tufas and travertines, Stateline area terrace and greenbed deposits, Crater Flat (Site 199) and the Lathrop Wells diatomite deposits, and Tertiary lacustrine limestones in the Amargosa Valley.

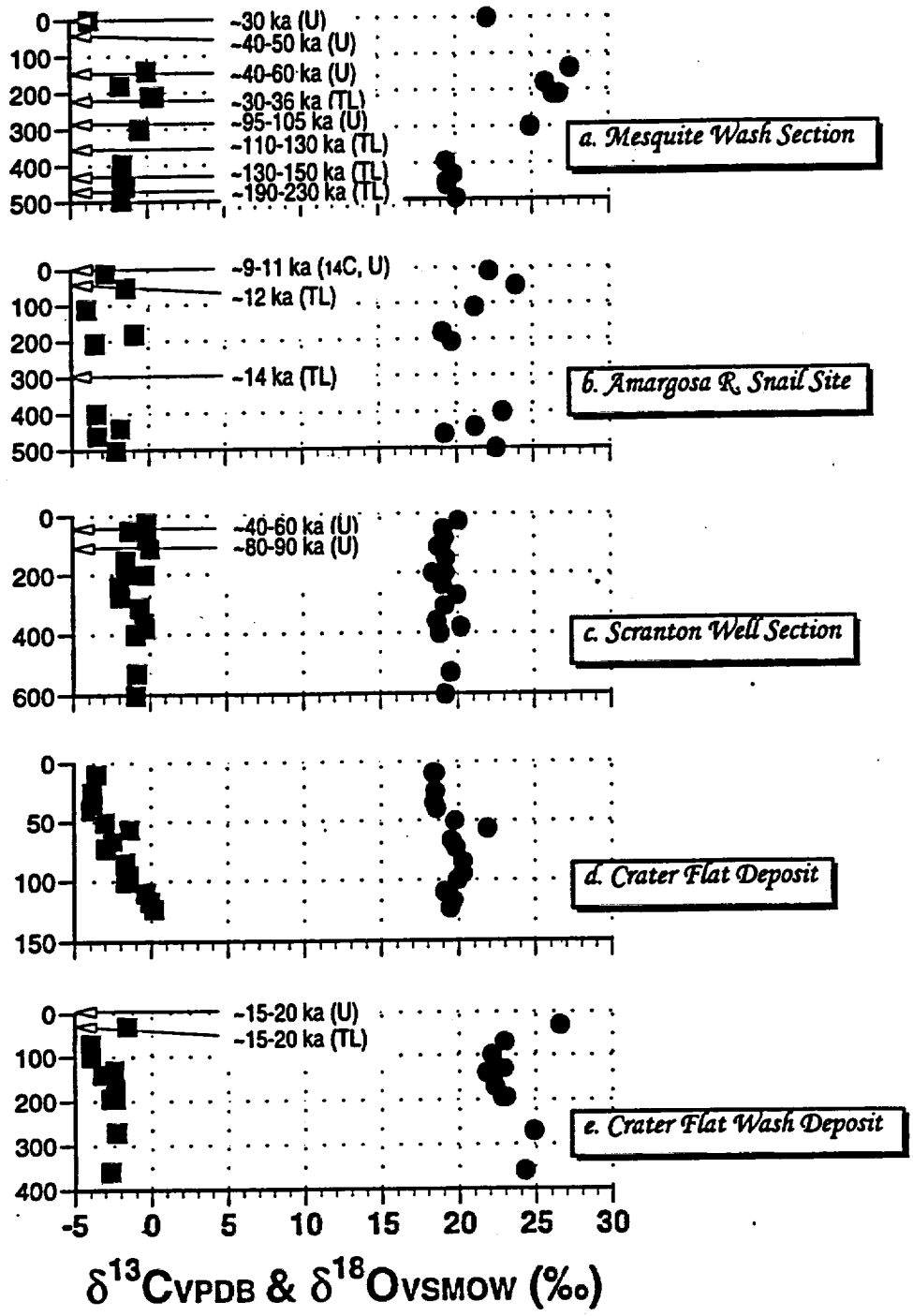

Fig. 6. Graphs of the $\delta^{13}C$ (■) and $\delta^{18}O$ (●) versus depth for the five hand-augured sections collected from paleo-discharge depositsduring FY1997. Depositional ages determined from these samples by $^{230}Th/U$, thermoluminescence, or radiocarbon techniques or depositional ages determined and reported during previous years are shown where possible.

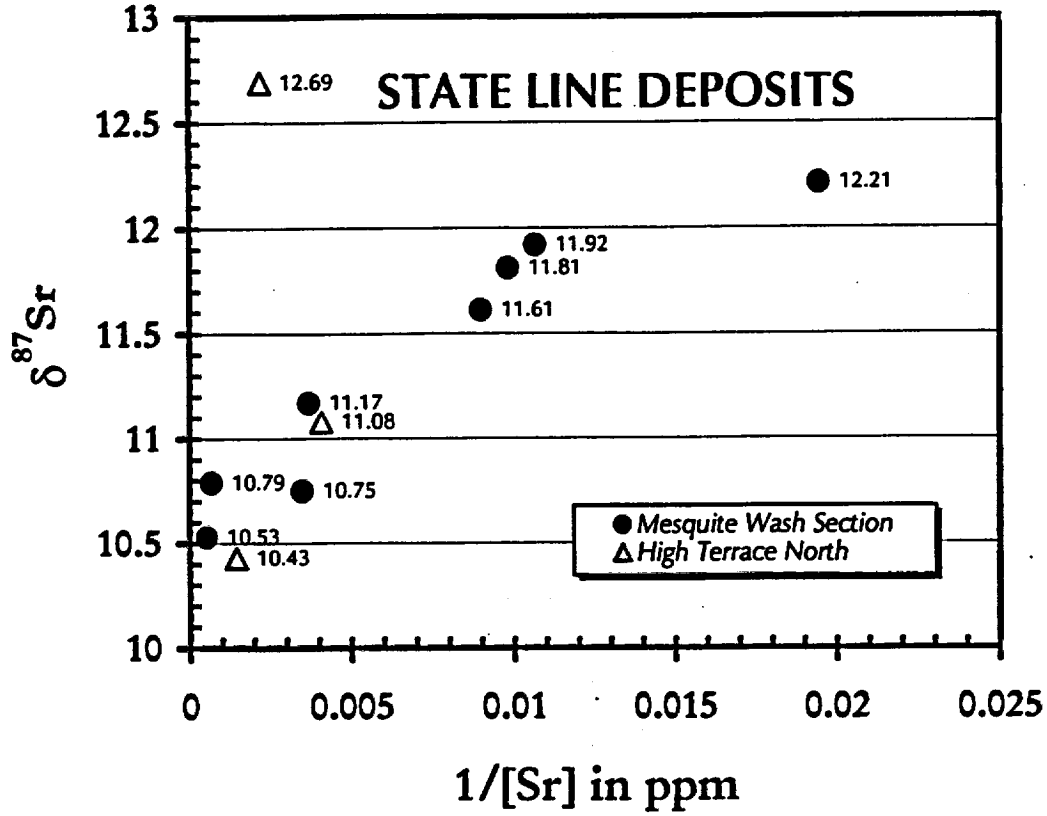

Figure 7: Correlation between Sr isotopic composition and inverse concentration for some carbonate-rich samples in the Mesquite Wash area of the State Line past discharge deposits. Values adjacent to symbols are d87Sr compositions given in Table 3.

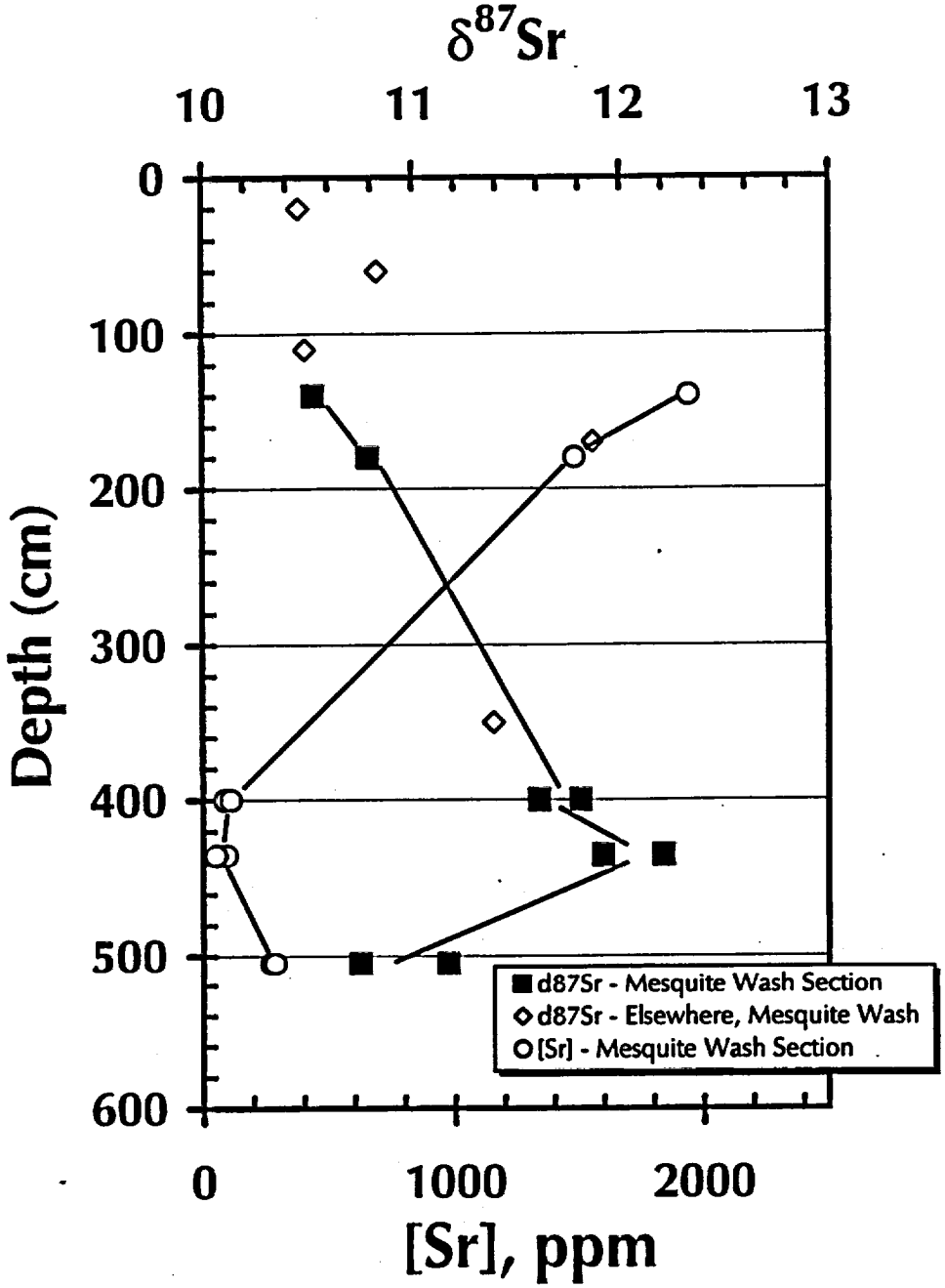

Figure 8: Variations of Sr isotopic composition and concentrations with depth in the Mesquite Wash section of the State Line discharge deposits. Data represented by open diamonds are from Paces (1995).

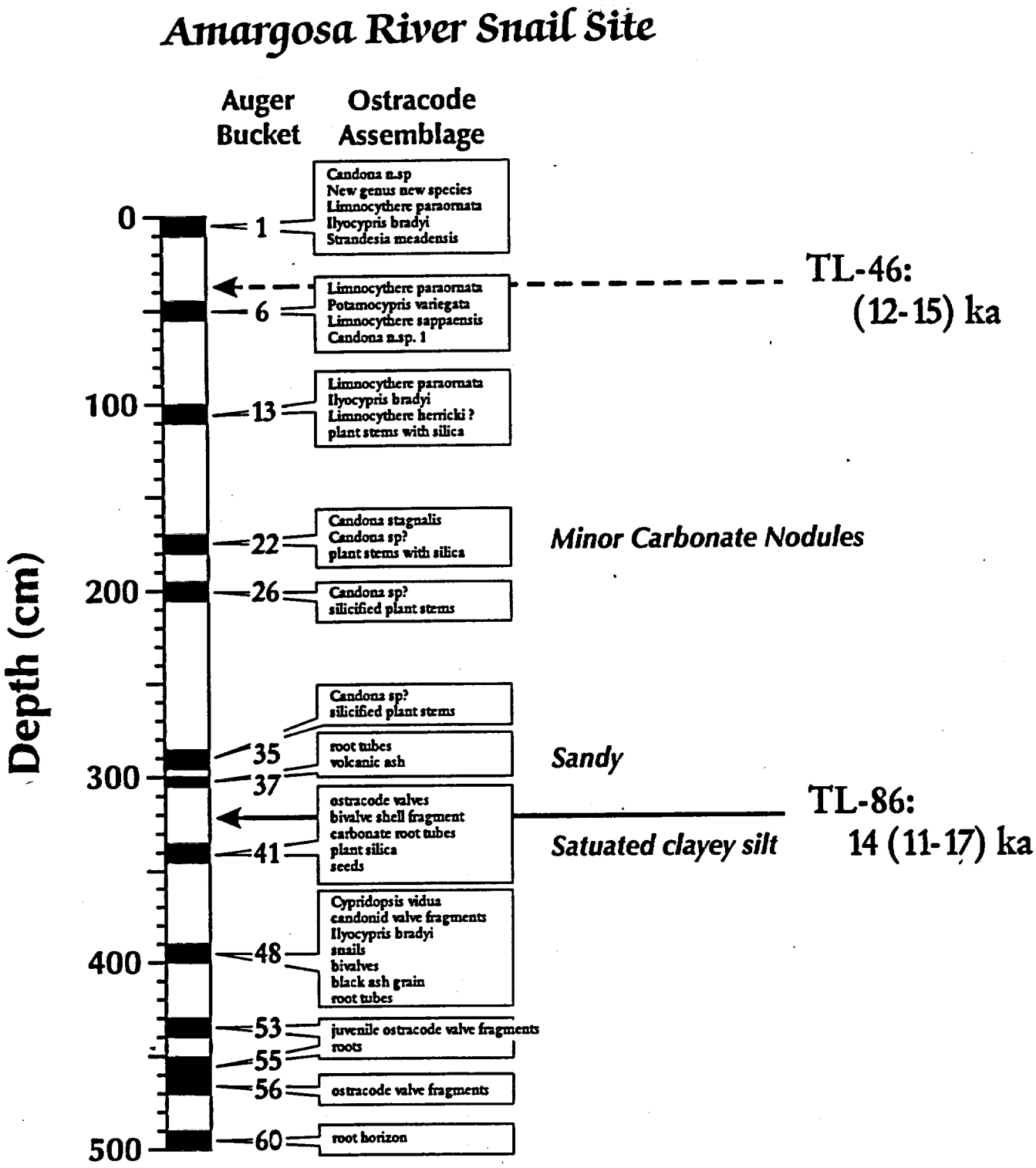

Figure 9: Schematic representation of auger hole showing sampled intervals, ostracode assembleges and TL ages (TL-46 data from Paces et al., 1996).

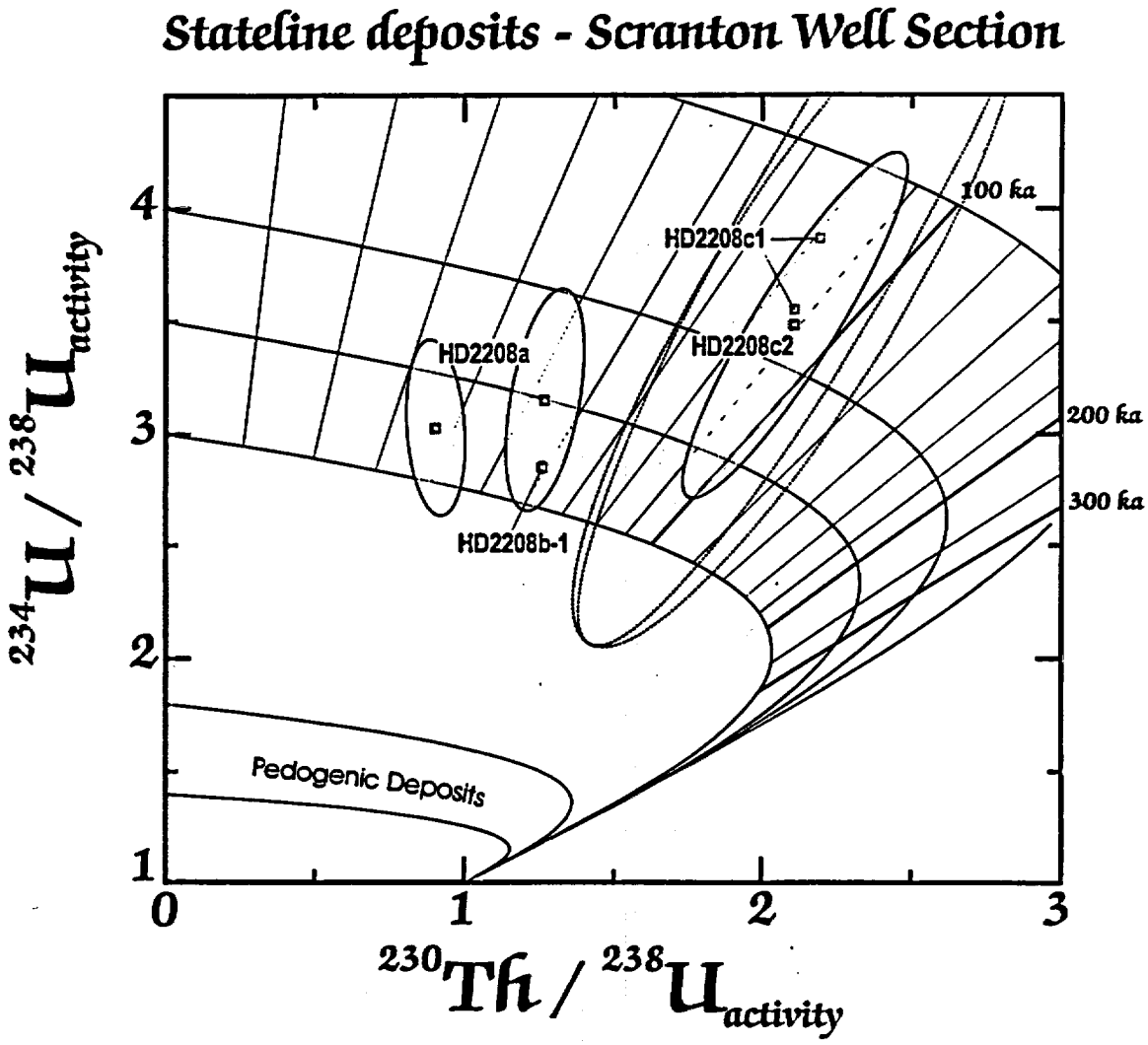

Figure 11: U-series evolution diagram showing U and Th isotopic results for data from Scranton Well.

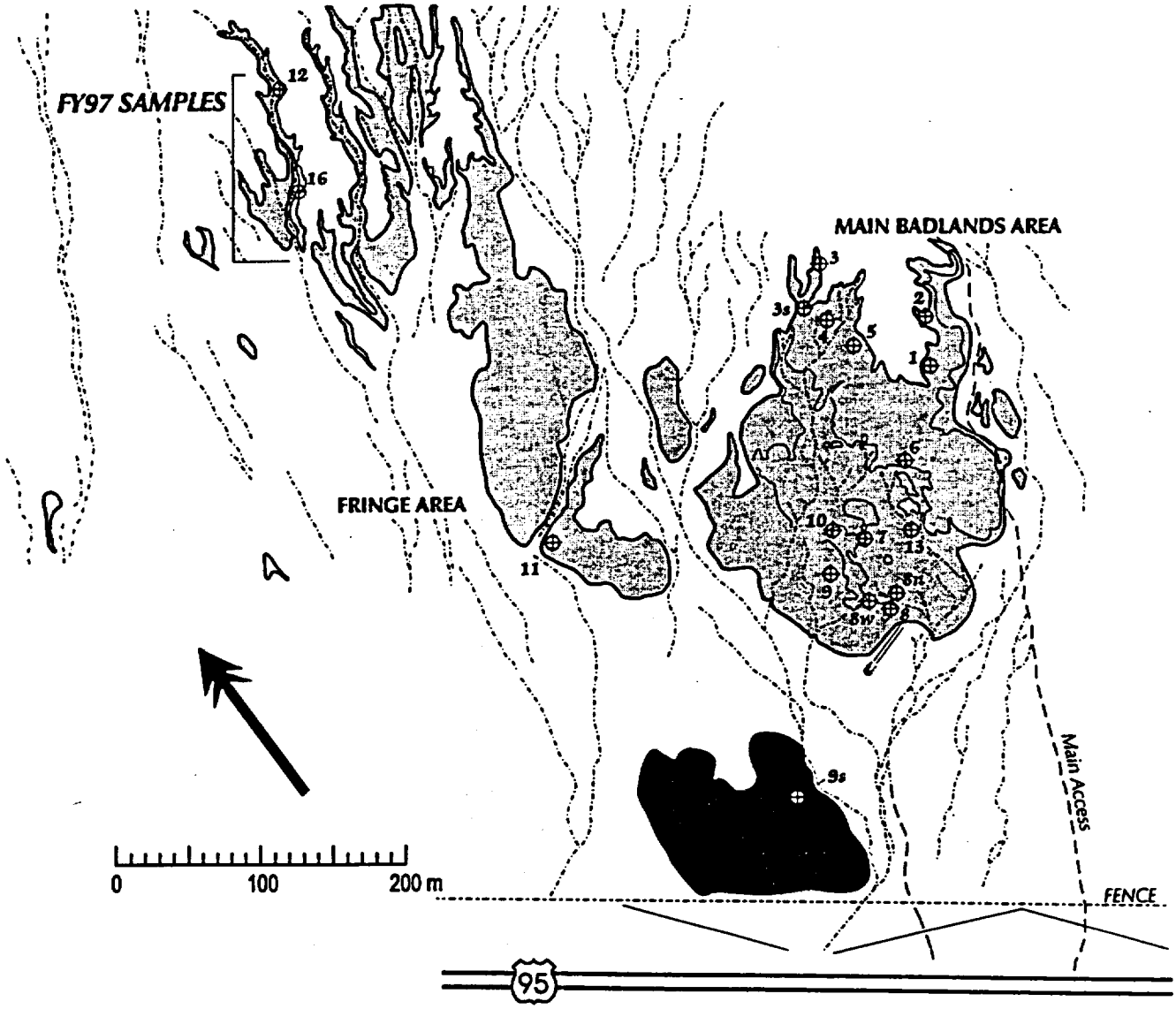

Figure 12: Sketch of air photos showing major morphologic features of the Lathrop Wells Diatomite deposit. Light-colored, fine-grained deposits are shown as light-shaded areas. Area with platy veneer of banded dense limestone shown with darker-shading. Numbered stations are shown with circle/cross symbol.

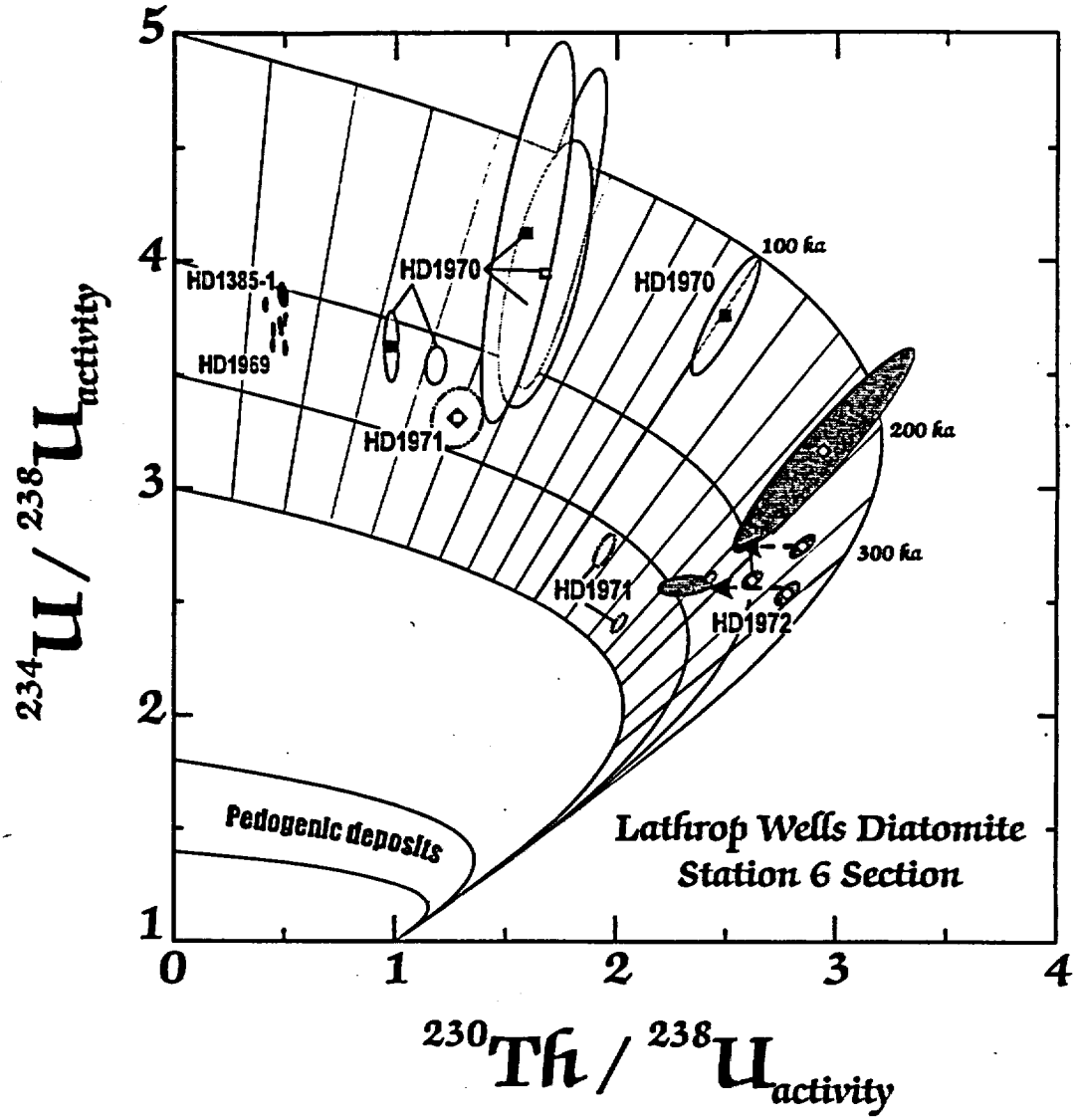

Figure 13: U-series evolution diagram showing U and Th isotopic data for analyses from LWD.

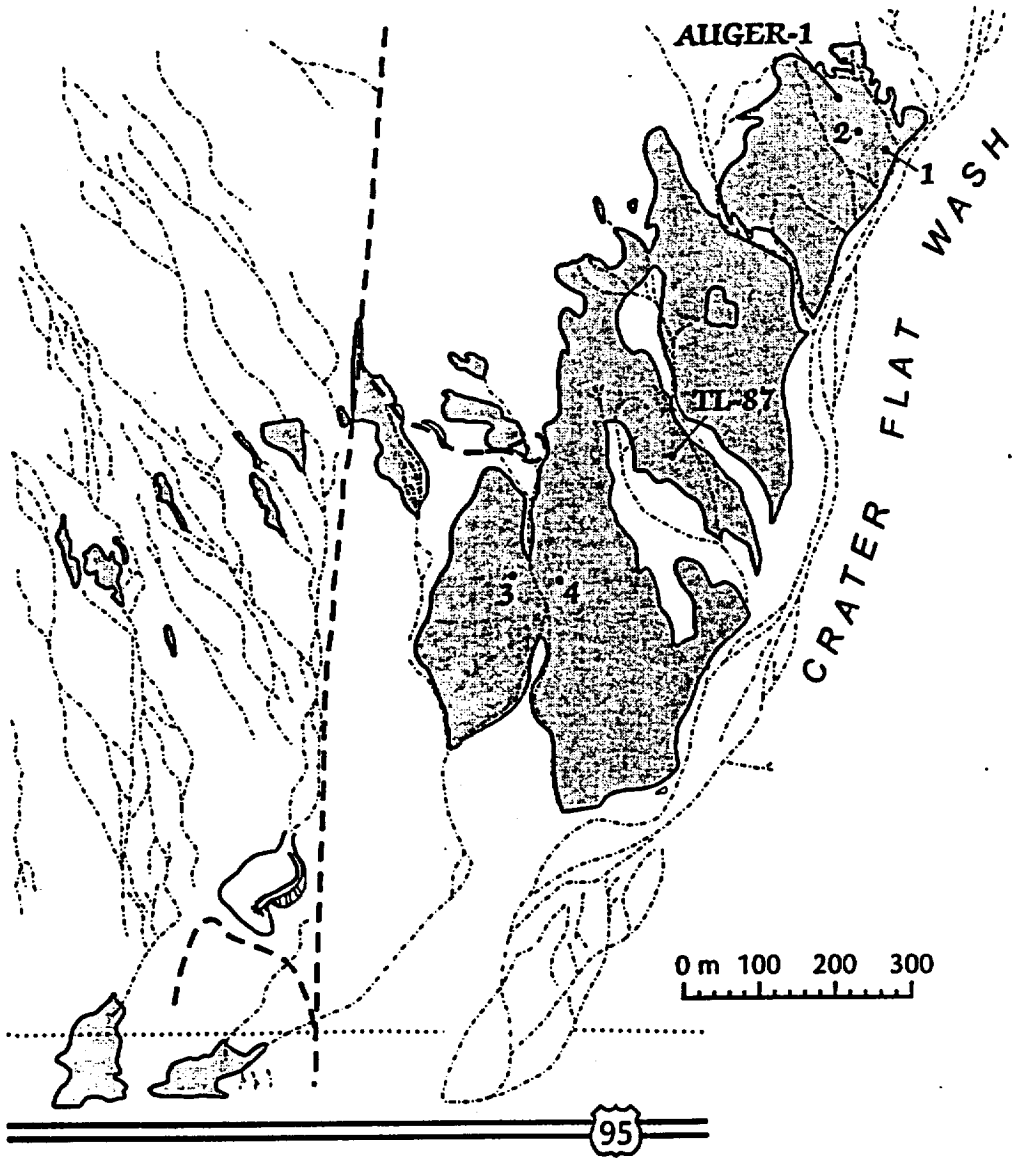

Figure 14: Sketch of air photos showing major morphologic features of the Crater Flat Wash deposit (CFW). Light-colored, fine-grained deoists are shown as light-shaded areas. Numbered sample stations are shown with small black circles.

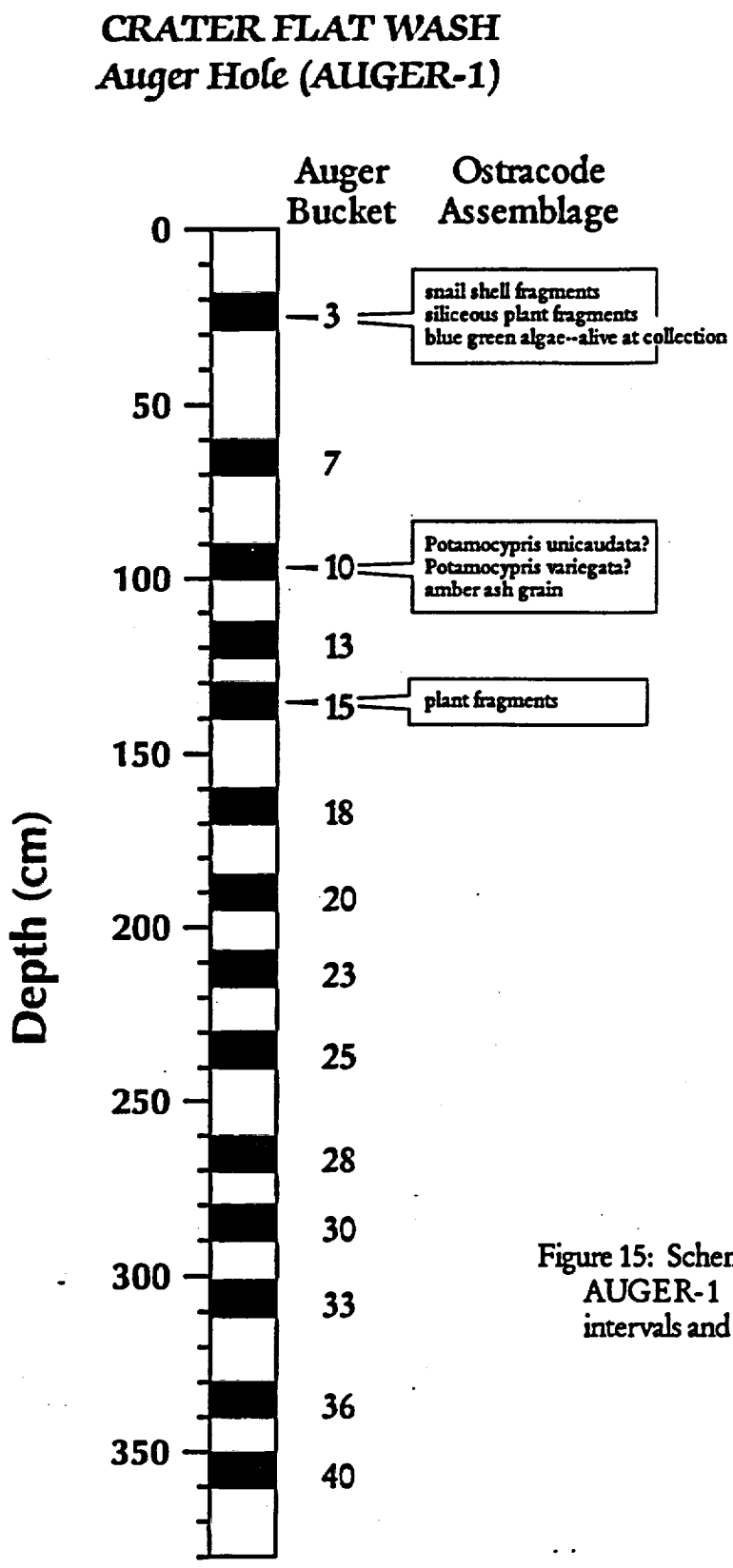

Figure 15: Schematic representation of CFW AUGER-1 hole showing sampled intervals and ostracode assembleges.

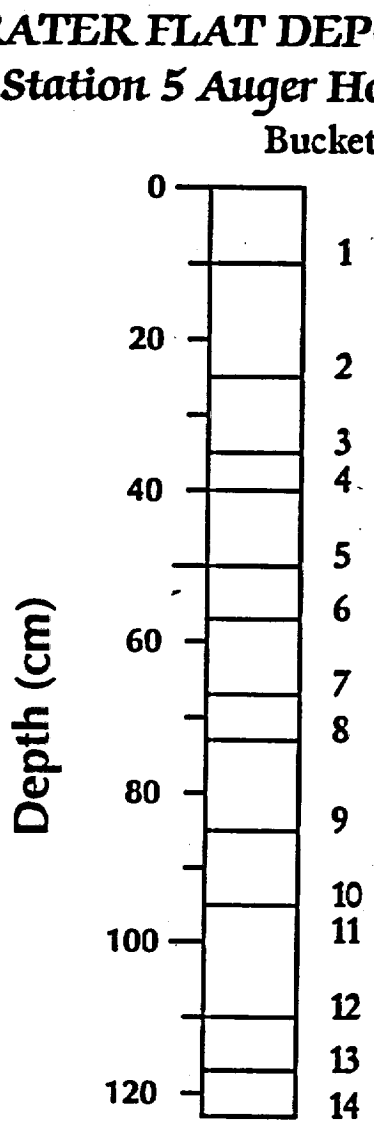

Figure 16: Schematic representation of continuously collected auger-bucket samples from CFD Station 5 auger hole.

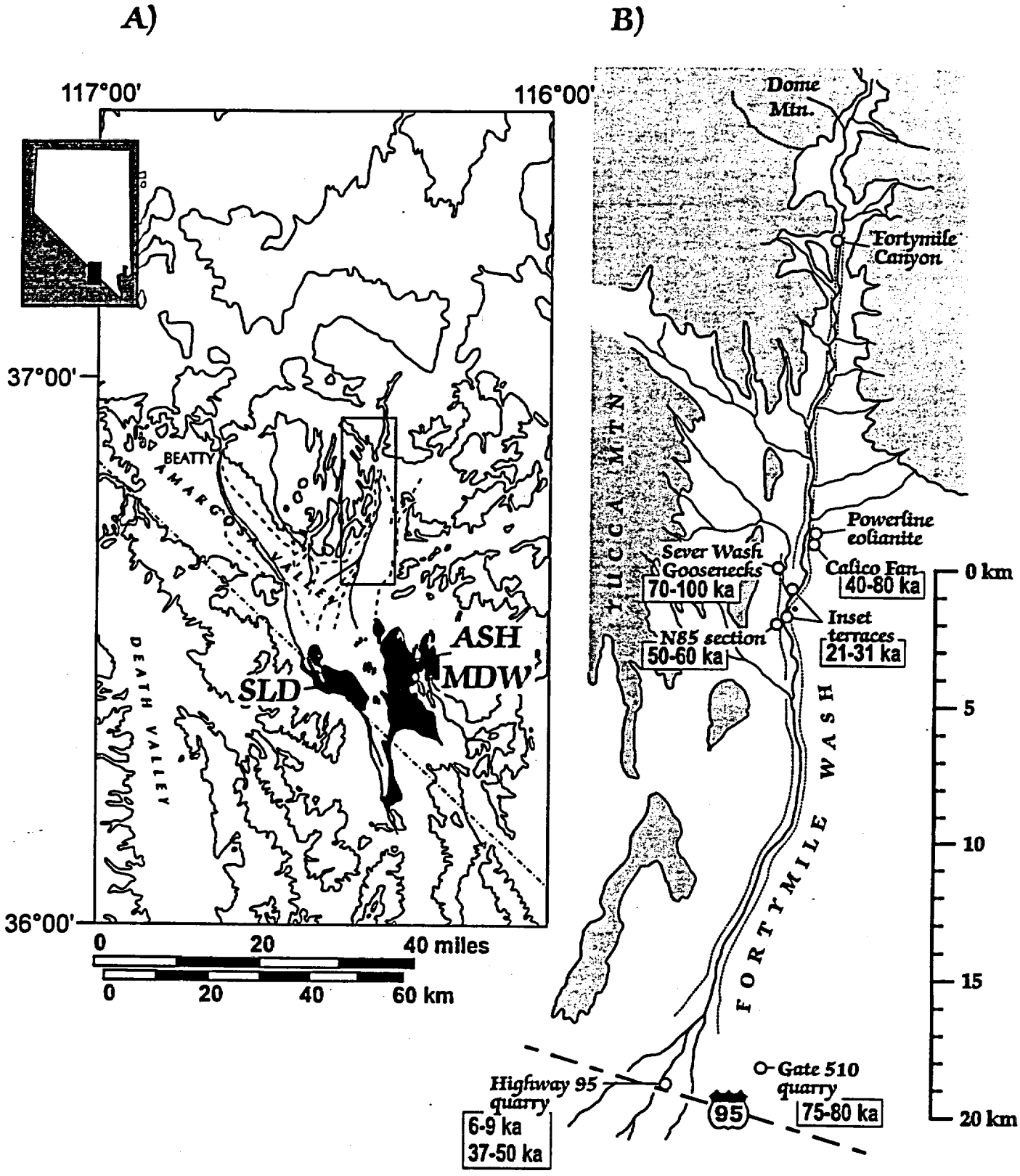

Figure 17: A) General geomorphic map of the southern Nevada and Eastern California showing the Fortymile Wash drainage system along with Quaternary discharge deposits in the southern Amargosa valley. B) Upper portion of the Fortymile Wash showing sites sampled for dating. Solid lines represent active ephemeral channels. Dotted lines represent arroyo walls incised into surrounding fan surface.

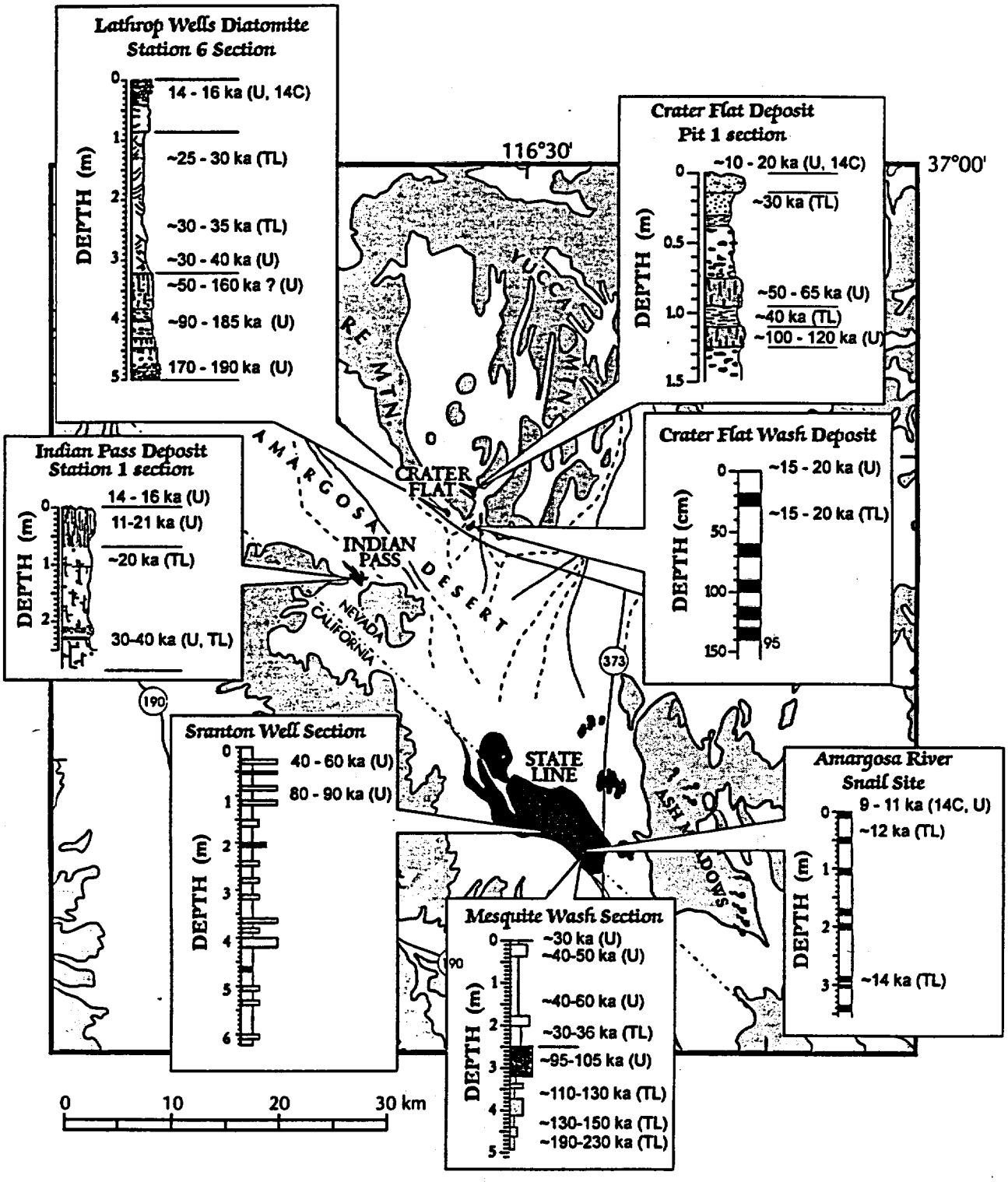

Figure 18: Stratigraphic and geochronologic framework of ground water discharge deposits in the Amargaso Desert and adjoining areas. Data are generallized from this report and from Paces and others (1996). Base map as in Figure 1.